POLITECNICO DI TORINO

INGEGNERIA PER L'AMBIENTE E IL TERRITORIO

Track: Industrial Environmental Sustainability

Department of Environment, Land and Infrastructure Engineering (DIATI)

Valorization of textile waste for sustainable composite construction material

Supervisor:

BELLOPEDE ROSSANA (DIATI)
FANTILLI ALESSANDRO PASQUALE (DISEG)
AKYILDIZ SINEM HAZAL (DIATI)

Written by:

KHAKPOOR SINA

A.A. 2025/2026

Acknowledgments

I would like to express my sincere gratitude to Prof. Rossana Bellopede for her continuous guidance, valuable advice, and encouragement throughout this thesis. Her availability and feedback were essential in shaping the direction of the work and completing the experimental activities.

I also sincerely thank Prof. Alessandro Pasquale Fantilli for his supervision, constructive suggestions, and academic guidance during the development of this thesis.

I am grateful to Sinem Hazal Akyıldız for her advice and assistance with the experimental work and the interpretation of the materials investigated in this study.

I would also like to thank everyone who assisted with the preparation, testing, and observation of the mortar specimens. Their help and availability contributed significantly to the completion of the experimental part of this research.

My thanks also go to my professors, classmates, and colleagues for their discussions, encouragement, and support throughout my studies.

Most importantly, I thank my family for their unconditional love, patience, and constant support. Even from a distance, their encouragement gave me the motivation to continue and complete this important stage of my academic journey.

Abstract

Textile-processing wastewater can contain heterogeneous fibers and fiber fragments. Recovering this material may create a secondary-material route, but its performance in cementitious matrices must be established experimentally. This thesis presents a preliminary evaluation of wastewater-recovered textile fibers (RTF) incorporated into cementitious mortar.

One hundred selected fibers were examined by optical and ultraviolet-light microscopy to describe color, fluorescence response, visual morphology, and length. The same recovered material batch had previously been characterized by micro-FTIR in Akyıldız et al. (2025b); micro-FTIR was not repeated in this thesis. Nine 40 × 40 × 160 mm mortar prisms were cast sequentially from one common base-mortar batch: Control specimens first without RTF, Layered specimens second with a localized fiber-rich region, and Mixed specimens last after RTF was incorporated into the remaining mortar. The RTF-containing groups retained the nominal 1 wt% experimental designation used in the laboratory plan; exact realized group-wise wt% cannot be independently reconstructed because the common batch was not weighed after sequential allocation. Flexural testing was performed at 56 days, compression testing of the resulting paired half-prisms at 116 days, and qualitative digital-microscope observations at 95 days.

The recovered material was visibly and dimensionally heterogeneous. The 100 fibers had lengths from 0.255 to 19.333 mm (mean 4.229 mm; median 2.544 mm). Visual morphology classified 63% as synthetic-like and 37% as natural-like; these categories are not quantitative polymer-composition results. Descriptive mean flexural strengths were 7.42 MPa for Control (n = 2 valid results), 7.28 MPa for Mixed (n = 3), and 7.80 MPa for Layered (n = 3, provisional because an improperly failed Layered specimen was not identified). Unfiltered descriptive mean compressive strengths were 55.82, 57.28, and 46.83 MPa, respectively, from six paired half-prisms derived from three parent prisms per group.

The numerical differences are descriptive and do not establish a strengthening effect. Selected two-dimensional fields showed localized fiber-rich zones in Layered specimens and more dispersed fiber-like elements in Mixed specimens, but did not quantify three-dimensional distribution, porosity, bond strength, or interfacial chemistry. Under the investigated conditions, the Mixed configuration provided the more balanced descriptive mechanical response. The use of one common mortar batch with sequential group allocation, the small specimen set, paired compression results, qualitative microscopy, and incompletely documented layer geometry restrict broader conclusions.

Keywords: textile wastewater; recovered textile fibers; material valorization; cementitious mortar; fiber placement; flexural strength; compressive strength; optical microscopy

Table of Contents

Acknowledgments *1*

Abstract *2*

Table of Contents *3*

List of Abbreviations *6*

1. Introduction *7*

1.1 Background and Motivation **7**

1.2 Problem Statement **7**

1.3 Aim and Objectives **8**

1.4 Scope of the Thesis **8**

1.5 Structure of the Thesis **9**

2. Literature Review *10*

2.1 Textile Waste, Microfiber Release, and Environmental Relevance **10**

2.1.1 Textile Waste Streams and Circular Management 10

2.1.2 Sources and Characteristics of Textile Microfibers 11

2.1.3 Environmental and Policy Context 12

2.2 Textile Microfibers in Wastewater Treatment **13**

2.2.1 Occurrence, Concentrations, and Removal 13

2.2.2 Partitioning to Sludge and Recovery Streams 14

2.2.3 Characterization and Polymer Composition 15

2.2.4 Recovery and Reuse Potential 17

2.3 Textile-Derived Fibers in Cementitious Materials **17**

2.3.1 Potential Reinforcement Mechanisms 17

2.3.2 Fresh-State Behavior and Dispersion 18

2.3.3 Flexural and Compressive Performance 19

2.3.4 Durability and Fiber–Matrix Interaction 19

2.4 Influence of Fiber Dosage and Placement Configuration **20**

2.4.1 Fibers Incorporated through Mixing 20

2.4.2 Layered and Localized Placement 21

2.4.3 Relevance to Wastewater-Derived RTF 21

2.5 Research Gap and Positioning of the Present Study **22**

3. Materials *23*

3.1 Recovered Textile Fibers **23**

3.1.1 Source, Recovery, and General Description 23

3.2 Cement **24**
3.3 Standard Sand **24**
3.4 Mixing Water **24**
3.5 Mortar Mix Design **24**
3.6 Specimen Groups and Identification **25**
4. Experimental Methods ***27***
4.1 Experimental Program and Chronology **27**
4.2 Characterization of Recovered Textile Fibers **27**
4.3 Preparation of Mortar Specimens **29**
4.4 Mixing Procedure **30**
4.5 Casting and Compaction **32**
4.6 Demolding and Curing **32**
4.7 Mechanical Testing Sequence and Actual Ages **33**
4.8 Flexural Strength Test **33**
4.9 Compressive Strength Test **35**
4.10 Digital-Microscope Observation of Mortar Specimens **38**
5. Results ***38***
5.1 Characterization Results of Recovered Textile Fibers **38**
5.1.1 Color Distribution 39
5.1.2 Fluorescence Response 39
5.1.3 Apparent Material Type Distribution 40
5.1.4 Fiber Length Distribution 40
5.1.5 Microscopic Appearance of Recovered Textile Fibers 41
5.2 Qualitative Handling Observations **42**
5.3 Flexural Strength Results **42**
5.4 Qualitative Digital-Microscope Observations **44**
5.4.1 Reference Specimens 44
5.4.2 Layered 1% RTF Specimens 46
5.4.3 Mixed 1% RTF Specimens 47
5.5 Compressive Strength Results **48**
5.5.1 Individual Compressive Strength Results 49
5.5.2 Comparison of Mean Compressive Strength 50
5.5.3 Failure Mode Observations 51

6. Discussion *53*
6.1 Feedstock Heterogeneity **53**
6.2 Handling and Incorporation **54**
6.3 Flexural Response **54**
6.4 Digital-Microscope Observations **54**
6.5 Compressive Response **55**
6.6 Combined Interpretation **55**
6.7 Comparison with Previous Studies **55**
6.8 Limitations **56**
7. Conclusions and Future Work *56*
7.1 Main Conclusions **57**
7.2 Practical Implications **57**
7.3 Future Work **57**
References *59*
Appendix *63*
Appendix A — Supplementary RTF Characterization Images **63**
Appendix B — Supplementary Specimen Preparation and Mechanical Testing Images **66**
Appendix C — Supplementary Digital-Microscope Observations **72**
C.1 Control Specimens 73
C.2 Layered 1% RTF Specimens 74
C.3 Mixed 1% RTF Specimens 75

List of Abbreviations

Term	Definition
BSI	British Standards Institution
CEN	European Committee for Standardization
EDS	energy-dispersive X-ray spectroscopy
EN	European Standard
FTIR	Fourier-transform infrared spectroscopy
ITZ	interfacial transition zone
LCA	life-cycle assessment
MPa	megapascal
PET	polyethylene terephthalate
RTF	recovered textile fibers
SD	sample standard deviation
SEM	scanning electron microscopy
UV	ultraviolet
w/c	water-to-cement mass ratio
wt%	mass percentage
WWTP	wastewater treatment plant
A	loaded compression area, mm^2
b	measured prism width, mm
d	measured prism depth at the flexural section, mm
F_c	maximum compressive load, N or kN as stated
F_f	maximum flexural load, N
l	flexural support span, mm
R_c	compressive strength, MPa
R_f	flexural strength, MPa

1. Introduction

1.1 Background and Motivation

The textile industry requires substantial quantities of water, energy, and raw materials and generates both solid waste and fiber-containing wastewater. During textile manufacturing and wet-processing operations, fibers can be released through mechanical and chemical stresses associated with washing, dyeing, finishing, brushing, raising, and material handling. These fibers may enter industrial wastewater-treatment systems, where part of the load is retained in sludge, filtration residues, or other solid streams, while a residual fraction may remain in treated effluent (Niinimäki et al., 2020; Ramasamy et al., 2022; Wang et al., 2023).

Fibrous material separated from textile-processing wastewater is generally managed as a waste or treatment residue. Depending on its properties and recovery route, however, it may represent a secondary material resource. Recovery and reuse can provide an alternative to disposal, but they do not automatically deliver an environmental benefit. The outcome depends on recovery, cleaning, drying, transport, manufacture, displacement of virgin materials, and end-of-life management (Sandin and Peters, 2018; Wang and Salmon, 2022).

The construction sector offers one possible outlet for recovered textile materials. Previous studies involving recycled PET, carpet waste, production residues, and other solid textile wastes show that fibers can affect fresh-state behavior, crack development, flexural response, toughness, and compressive performance. These effects depend on source, geometry, dosage, distribution, surface condition, and matrix quality, and cannot be transferred automatically to heterogeneous fibers recovered from wastewater (Rahman et al., 2022; Sasi et al., 2024; Tran et al., 2022).

This context provides the motivation for the present study. The thesis investigates the incorporation of textile fibers recovered from textile wastewater into cementitious mortar as a potential material-valorization route. It specifically examines whether the selected recovered material can be incorporated at a defined dosage and whether its placement within the mortar is associated with differences in the observed mechanical response and internal appearance.

1.2 Problem Statement

Most studies of textile-derived fibers in cementitious materials concern garments, carpets, industrial offcuts, recycled PET, or purpose-made textile reinforcement. Relatively few address loose fibers recovered directly from textile-processing wastewater. Such material can differ in composition, cleanliness, geometry, surface condition, entanglement, and residues from textile processing (Akyıldız et al., 2022; Akyıldız et al., 2025a; Ramasamy et al., 2022).

These differences create uncertainty about incorporation and performance. Dosage alone cannot predict the response: mixing, spatial distribution, local concentration, compaction, matrix penetration, and fiber–matrix interaction may also matter. Mechanisms reported for conventional fiber-reinforced materials provide hypotheses, not proof for the RTF investigated here (Peled and Bentur, 2000; Sadrolodabaee et al., 2021a; Tran et al., 2022).

A further uncertainty concerns incorporation. Mixing aims to distribute loose fibers throughout the mortar, whereas layered placement concentrates an intended nominal fiber addition in a local internal region. The two configurations may influence flexural and compressive response differently, but direct evidence under the same nominal dosage designation for wastewater-recovered RTF is limited.

The experimental question is therefore whether the selected RTF can be incorporated under the nominal 1 wt% experimental condition and whether Mixed and Layered placement are associated with different descriptive mechanical results and qualitative microscopic features.

1.3 Aim and Objectives

The aim is to provide a preliminary experimental evaluation of textile fibers recovered from textile wastewater as a secondary constituent in cementitious mortar.

The specific objectives are:

- to establish the environmental and circular-economy context for recovering and potentially valorizing textile fibers from industrial wastewater;
- to characterize the selected RTF by color, fluorescence response, visual morphology, and fiber length;
- to prepare a Control group and two nominal 1 wt% RTF groups, incorporated by mixing and by localized layered placement, from a common base-mortar batch;
- to evaluate the parent prisms in three-point flexure and the resulting paired half-prisms in compression;
- to compare selected fractured and cut surfaces by qualitative digital-microscope observation;
- to compare the descriptive mechanical and visible internal responses associated with the two placement configurations;
- to identify the principal limitations and define priorities for controlled follow-up research.

1.4 Scope of the Thesis

The study characterizes the selected RTF physically; tests mortar prisms in three-point flexure and their resulting half-prisms in compression and uses qualitative digital-microscope observations of selected fractured and cut surfaces. Mechanical analysis is limited to recorded peak strengths; microscopy is used only to describe visible features.

The program is preliminary and configuration focused. It does not optimize dosage, develop a structural-concrete product, or propose RTF as a substitute for conventional reinforcement. It does not measure load–deflection behavior, fracture energy, residual strength, standardized flow, fresh density, air content, or quantitative porosity. The same recovered material batch had previously been characterized by micro-FTIR in Akyıldız et al. (2025b), but micro-FTIR was not repeated as part of the present thesis. Optical, ultraviolet-light, and digital-microscope

observations were not used to assign chemical identity. SEM/EDS and other high-resolution interface analyses were not performed.

The environmental rationale is addressed conceptually. A life-cycle assessment is outside the scope because reliable inventories for recovery, conditioning, transport, production, and end-of-life management were unavailable. Durability and application-specific performance were likewise not assessed.

1.5 Structure of the Thesis

The thesis is organized into seven chapters.

Chapter 1 introduces the background, motivation, research problem, aim, objectives, and scope of the study.

Chapter 2 reviews textile-waste streams, fiber release, occurrence and recovery in wastewater systems, and textile-derived fibers in cementitious materials. It distinguishes the previously published same-batch micro-FTIR results from the visual characterization performed in this thesis.

Chapter 3 describes the RTF source and prior conditioning, cement, standard sand, nominal water, mix design, and specimen groups.

Chapter 4 presents fiber characterization, mortar preparation, casting, curing, flexural testing, compression testing, and qualitative digital-microscope observation.

Chapter 5 reports the fiber-characterization, qualitative handling, mechanical, and microscopic results.

Chapter 6 interprets the descriptive findings in relation to feedstock heterogeneity, incorporation, previous research, and experimental limitations.

Chapter 7 states the conclusions, conservative practical implications, and priorities for future work. Appendices provide supplementary images.

2. Literature Review

This chapter develops the rationale for recovering textile fibers from industrial wastewater and evaluating them as a secondary constituent in cementitious mortar. It distinguishes solid textile waste, wastewater microfiber pollution, wastewater-recovered fibers, and engineered textile reinforcement before positioning the present experiment within the evidence gap.

2.1 Textile Waste, Microfiber Release, and Environmental Relevance

Textile circularity includes both solid waste and fibers released into process water. These streams have different origins, compositions, and recovery constraints. Wastewater-recovered RTF therefore require separate consideration from conventional textile scraps, post-consumer garments, or purpose-made reinforcement.

2.1.1 Textile Waste Streams and Circular Management

Textile waste is commonly classified as pre-consumer or post-consumer according to the point at which it leaves the product system. Pre-consumer waste is generated during fiber, yarn, fabric, and garment manufacture and includes offcuts, yarn residues, defective products, and other production losses. Post-consumer waste comprises garments, household textiles, and related products discarded after use. Compared with many pre-consumer streams, post-consumer textiles are generally more heterogeneous because they can contain fiber blends, dyes, finishes, accessories, wear-related contamination, and incomplete composition information (Das et al., 2025; Juanga-Labayen et al., 2022; Tang, 2023).

Recovery options depend on both stream quality and the intended output. Relatively clean and compositionally controlled production waste may be suitable for mechanical recycling or direct incorporation into secondary products, whereas mixed post-consumer waste often requires more intensive collection, sorting, and preparation. Across both categories, fiber blends, degraded material quality, contamination, and weak markets for secondary fibers can restrict closed-loop textile-to-textile recycling (Mohtaram and Fojan, 2025; Shirvanimoghaddam et al., 2020; Wang and Salmon, 2022).

When closed-loop recycling is not technically or economically feasible, open-loop recycling or material valorization may retain some material utility by incorporating the recovered material into a different product system. Such routes do not automatically provide an environmental benefit; performance, processing demand, displacement of virgin material, and end-of-life consequences remain relevant. Nevertheless, reviews of textile recycling and construction applications identify insulation, cementitious composites, and other building products as possible outlets for textile-derived secondary materials (Biyada et al., 2023; Rahman et al., 2022; Sandin and Peters, 2018).

The present thesis concerns fibers recovered from industrial textile-processing wastewater. Solid pre-consumer and post-consumer wastes provide context but are not direct equivalents of the experimental material. The question is whether a heterogeneous wastewater-derived residue can be incorporated into cementitious mortar as a potential valorization route.

2.1.2 Sources and Characteristics of Textile Microfibers

Textile fibers can be released during manufacture, use, laundering, and end-of-life handling. Within production facilities, shedding may occur during fabric formation, pretreatment, dyeing, washing, finishing, and internal material transport. Evidence from polyester production and industrial monitoring shows that release depends on the textile construction and on the mechanical and chemical stresses applied during processing; it cannot be represented by a single emission factor for all plants or products (Cai et al., 2020; Wang et al., 2023; Zhang et al., 2021).

Mechanical finishing is particularly relevant to wastewater-derived fiber recovery. Raising, brushing, sueding, and related operations abrade the fabric surface to create a desired handle or appearance and can detach short fiber fragments. Plant-scale studies have recovered and identified fibers directly from textile-company wastewater and from the discharge of finishing equipment, confirming that production-stage wastewater is an important point source (Akyıldız et al., 2022; Akyıldız et al., 2024).

The composition of an industrial microfiber stream reflects the materials processed at the facility. Studies of textile wastewater have reported synthetic fibers such as polyester, acrylic, polyamide, and polypropylene together with cotton, wool, viscose, rayon, and other cellulose-based materials. Relative abundance varies among plants, sampling points, and analytical methods, so a composition reported for one facility should not be transferred to another without direct identification (Akyıldız et al., 2022; Chan et al., 2023; Ramasamy et al., 2022).

Wastewater-derived fibers are heterogeneous in length, diameter, curvature, color, surface condition, and entanglement. Environmental studies often define microfibers operationally as fibrous particles shorter than 5 mm, although definitions and detection limits vary (Akyıldız et al., 2025a; Zhou et al., 2020). The material examined here ranged from 0.255 to 19.333 mm; therefore, the complete experimental feedstock is termed ‘recovered textile fibers’ rather than a strict microfiber fraction.

This variability matters for reuse because industrial practice requires reasonably consistent properties and performance. Commercial reinforcing fibers are normally specified by polymer, geometry, tensile properties, and surface condition, whereas wastewater-recovered RTF may contain several fiber families and a broad geometry distribution. Their dispersion and interaction with mortar must therefore be assessed experimentally (McCay and Mehta, 2024; Ramasamy et al., 2022).

2.1.3 Environmental and Policy Context

Textile production has environmental burdens across raw-material supply, wet processing, product use, and end-of-life management. Water and chemical use, energy demand, greenhouse-gas emissions, solid waste, and fiber release occur at different stages and depend strongly on the textile product and production system. Broad sector reviews therefore support a life-cycle perspective while also warning against reducing the problem to one waste stream or one indicator (Fonseca et al., 2023; Niinimäki et al., 2020).

In 2022, the European Union textile value chain generated an estimated 159 Mt CO_2-equivalent (355 kg per person), while EU textile waste generation was approximately 6.94 Mt (16 kg per person). These sector-wide estimates indicate the scale of the resource and waste challenge but do not quantify the environmental performance of the mortar studied here (European Environment Agency, 2025).

Circular-economy strategies emphasize waste prevention, longer product use, reuse, repair, recycling, and improved material traceability. In the European Union, the waste framework has been amended to strengthen requirements related to textiles, including extended producer responsibility and improved collection and treatment (European Parliament and Council of the European Union, 2025). Reviews nevertheless identify continuing barriers associated with mixed materials, collection quality, sorting capacity, and markets for recovered fibers (Wojnowska-Baryła et al., 2024).

Microfiber release adds a water-pollution dimension to textile circularity. Industrial wastewater treatment can lower fiber concentrations, but residual discharge remains possible and captured material may be transferred to sludge or other solid residues. Treatment therefore changes the location and concentration of the fibers; it does not by itself establish safe final management or beneficial reuse (Chan et al., 2023; McCay and Mehta, 2024; Ramasamy et al., 2022).

Recovering a sufficiently clean fiber-rich stream before final discharge may connect pollution control with resource recovery. The environmental benefit of any reuse route would require a system-level assessment that includes recovery, cleaning, drying, transport, product performance, and end-of-life management. Such an assessment is outside the present thesis. Here, circularity provides the rationale for a preliminary material evaluation rather than a quantified claim of environmental superiority.

2.2 Textile Microfibers in Wastewater Treatment

Industrial wastewater studies show that microfiber abundance and composition vary with the processed textiles, production operations, sampling location, treatment train, and analytical protocol. This section reviews those differences, the partitioning of fibers into liquid and solid streams, the methods used for identification, and the implications for recovery.

2.2.1 Occurrence, Concentrations, and Removal

Textile wet-processing wastewater can contain higher microfiber counts than many reported municipal effluents because fibers are released directly during production. The available industrial evidence is heterogeneous: some studies sampled individual process discharges, others sampled on-site treatment inflow and outflow, and others examined centralized plants receiving wastewater from multiple textile mills. Sample volume, pretreatment, filter pore size, size cutoff, counting method, and polymer-confirmation rate also differ, which limits direct comparison (Chan et al., 2021; Chan et al., 2023; Ramasamy et al., 2022).

Table 2.1 summarizes four primary industrial studies. The values are retained on the basis reported by each source rather than normalized across incompatible methods.

Table 2.1. Representative microfiber concentrations and reported removal in textile wastewater systems

Study and system	Sampling basis	Inflow or source stream (microfibers L^{-1})	Outflow or final effluent (microfibers L^{-1})	Reported removal and interpretation
Akyıldız et al. (2022): on-site physicochemical treatment at a textile company	Ten samples collected around treatment inflow and outflow	893–4,452	310–2,404	38–65% reduction across samples; reported ranges should not be treated as one paired mean
Akyıldız et al. (2025a): on-site treatment at an Italian textile dyeing company	Treatment inflow and outflow; sludge sampled separately	825	520	36.97% removal from the sampled water stream
Zhou et al. (2020): printing and dyeing wastewater and a centralized industrial-park WWTP	Maximum source-stream count and mean centralized final-effluent count; not a paired mass balance	Up to 54,100	537.5 (mean)	>85% treatment removal; the source and effluent values have different reported bases
Xu et al. (2018): textile dyeing wastewater treatment plant	Mean influent and final-effluent concentrations	334.1 ± 24.3	16.3 ± 1.2	95.1% decrease; residual release remained because of the plant flow rate

Note. Values and units are retained as reported by the original studies. Sampling location, particle-size cutoff, separation and identification method, and stream definition differ among studies; the values therefore support within-study interpretation rather than a standardized cross-study mass balance.

The table shows why removal percentage and residual concentration must be interpreted together. Akyıldız et al. (2022) reported wide inflow and outflow ranges across samples from one physicochemical treatment system. Akyıldız et al. (2025a) found only partial removal at a different textile dyeing facility. Zhou et al. (2020) reported very high counts in printing and dyeing wastewater and a substantial mean concentration in centralized final effluent even though treatment removal exceeded 85%. Xu et al. (2018) reported a 95.1% decrease but still calculated

a large daily discharge because of the plant flow rate. These studies differ in basis and should not be combined into a single universal concentration range or treatment efficiency.

More recent evidence likewise shows substantial plant-to-plant variation. Across textile effluent-treatment plants in Bangladesh, Haque et al. (2024) reported removal efficiencies ranging from 23.52% to 82.19%. Industrial effluent studies also show that fiber number, size distribution, and polymer composition can change across treatment stages, and that a high percentage removal does not imply zero release (Chan et al., 2021; Haque et al., 2024).

Size-selective removal remains method-dependent. Smaller fibers can be proportionally enriched in treated effluent and are especially sensitive to analytical cutoffs, but the reviewed evidence does not establish one universal 100 µm threshold for all conventional treatment systems (Chan et al., 2023; Zhou et al., 2020). Treatment performance should therefore be interpreted in relation to each study's reported size range and detection limit.

2.2.2 Partitioning to Sludge and Recovery Streams

During treatment, fibers may remain suspended, associate with flocs, settle with solids, or be retained by filtration and membrane processes. Studies of conventional activated sludge and membrane bioreactor systems show that a large fraction of microplastic particles and fibers can be transferred from the water phase to sludge or retained solids (Lares et al., 2018). Industrial textile studies similarly report fibers in both treated effluent and sludge, although concentrations and units are not directly comparable across matrices (Akyıldız et al., 2025a; Haque et al., 2024).

Consequently, a reduction in effluent count should be described as removal from the sampled water stream, not destruction of the fibers. Sludge and other captured solids can act as sinks during treatment and may become secondary pathways if they are subsequently handled, land-applied, stored, or disposed of without controls (McCay and Mehta, 2024; Ramasamy et al., 2022). This distinction is central to resource recovery because the concentrated solid stream may be more practical to collect than dilute final effluent, while also containing more nonfiber material.

Treatment technology influences the location and form of captured material. Primary clarification, biological treatment, tertiary filtration, dissolved air flotation, and membrane systems have all been evaluated for microliter or microplastic removal, but much of the detailed process evidence comes from municipal wastewater rather than textile-industrial plants (Lares et al., 2018; Talvitie et al., 2017). Advanced oxidation has also been tested for polyester microfibers under controlled conditions, yet such findings cannot be generalized to a heterogeneous industrial fiber residue without further evidence (Easton et al., 2023).

For reuse, the preferred recovery point is not necessarily the stage with the highest apparent removal. A source-specific filter residue may contain fewer biological and mineral solids than

mixed sludge, whereas coagulation or flotation residues may contain treatment chemicals and dye-rich flocs. Selection therefore requires information on fiber concentration, accompanying solids, moisture, chemicals, and downstream cleaning requirements. The present study evaluates an already recovered RTF stream; it does not optimize the wastewater-treatment or recovery process.

2.2.3 Characterization and Polymer Composition

The chemical and physical heterogeneity of wastewater-derived fibers affects both environmental monitoring and material reuse. Optical microscopy can describe count, apparent shape, color, curvature, fibrillation, and visible surface contamination, but visual appearance alone cannot identify polymer type reliably. Fluorescence can indicate dyes or optical brighteners, yet it is also insufficient for definitive chemical classification (Akyıldız et al., 2025a; Lares et al., 2018).

Spectroscopic methods are therefore used for polymer identification. Micro-FTIR can distinguish major polymer families when spectra and reference libraries are adequate, while Raman microscopy can complement FTIR for some small or strongly colored particles. Identification quality depends on sample preparation, particle size, filter compatibility, spectral acquisition, and interference from dyes or organic matter (Akyıldız et al., 2025a; Lares et al., 2018). These methodological dependencies partly explain differences among reported polymer profiles.

The recovered textile-fiber material used in the present thesis was obtained from the same material batch previously characterized by micro-FTIR spectroscopy in the study reported by Akyıldız et al. (2025b). That analysis identified acrylic, polyester, polypropylene, polyamide, cotton, viscose, and wool among the recovered fibers. Figure 2.1 reproduces the spectra reported in that study. These previously published results provide supporting chemical-characterization information for the material used in the present investigation. Micro-FTIR analysis was not repeated as part of this thesis, whose experimental program focused on incorporating the previously characterized material into cementitious mortar and evaluating the resulting specimens.

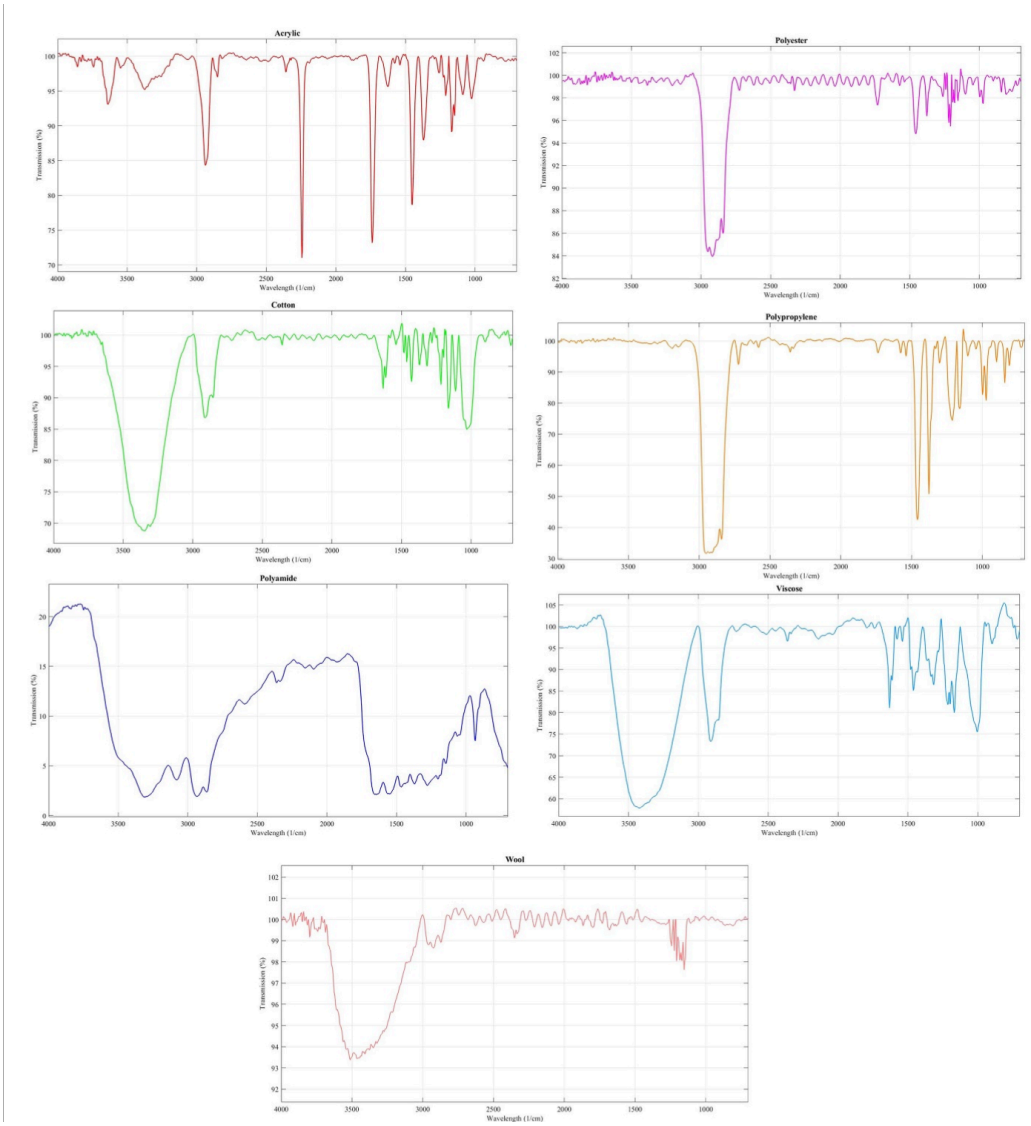


Figure 2.1. Micro-FTIR spectra of fiber types identified in the recovered textile-wastewater material. Reproduced from Akyıldız et al. (2025b) under CC BY 4.0.

Other plant-scale work has also identified mixtures of natural, regenerated, and synthetic fibers in textile wastewater (Akyıldız et al., 2022; Akyıldız et al., 2024). These findings demonstrate the compositional heterogeneity that may occur in wastewater-derived textile-fiber streams. For the material used in the present thesis, polymer composition was previously investigated by micro-FTIR spectroscopy, as reported by Akyıldız et al. (2025b). The optical, UV-light, and digital-microscope observations performed in the present thesis were used to describe fiber morphology, color, fluorescence response, length, and visible features of the mortar specimens. These observations were not used for polymer identification. Although microscopy can provide qualitative information about features visible on selected two-dimensional surfaces, it cannot quantify three-dimensional fiber distribution or orientation, porosity, or fiber–matrix interfacial chemistry.

2.2.4 Recovery and Reuse Potential

Potential recovery points include process-specific screening or filtration, on-site treatment solids, tertiary-filter backwash, flotation residues, and membrane concentrates. Recovery close to a high-shedding operation can reduce dilution and may avoid some contaminants introduced later in the treatment train. Akyıldız et al. (2024), for example, isolated fibers directly from finishing-process wastewater, while Akyıldız et al. (2022) compared separation approaches for samples collected around an on-site treatment plant.

Recovery does not by itself make the material suitable for reuse. Moisture, dyes, finishing chemicals, biological matter, mineral solids, fiber entanglement, and broad geometry can affect handling and compatibility with a new matrix. Cleaning and drying may improve consistency, but their material yield, chemical demand, energy use, and effect on fiber integrity must be evaluated for the intended application rather than assumed to be beneficial.

Akyıldız et al. (2025b) used the same recovered material batch in acoustic panels with a polyester binder, showing that thickness, density, and binder ratio affected sound absorption. This provides evidence of a non-structural valorization route but does not establish behavior in cementitious mortar.

A different material route was reported by Malchiodi et al. (2022), who incorporated textile-finishing waste into cement-based composites. Its feedstock and processing differ from the present wastewater-recovered RTF, so it provides a comparison rather than direct validation.

Construction-related reviews describe broader uses of textile waste in insulation and cement-based materials, but most of those feedstocks are solid production waste, garments, carpets, or purpose-made nonwovens (Biyada et al., 2023; Rahman et al., 2022). Incorporation of wastewater-derived RTF into mortar is more demanding because the fresh matrix must wet and surround a heterogeneous fiber population without creating unacceptable clustering or internal discontinuities.

2.3 Textile-Derived Fibers in Cementitious Materials

Research on textile-derived fibers in cementitious materials provides mechanisms and comparison points, but the literature includes materially different systems: commercial polymer fibers, fibers cut from recycled PET, processed garment or carpet waste, loose short fibers, nonwoven sheets, and engineered textiles. Their findings should be transferred to heterogeneous wastewater-recovered RTF only with caution.

2.3.1 Potential Reinforcement Mechanisms

Short fibers principally influence cementitious composites after matrix cracking. A fiber that intersects a crack and is adequately embedded can transfer stress between the crack faces,

restrict crack opening, and delay complete separation. This crack-bridging mechanism is well established across polymer-fiber and recycled-textile studies, but its efficiency depends on fiber geometry, orientation, distribution, and bond with the matrix (Rahman et al., 2022; Sasi et al., 2024; Tran et al., 2022).

The contribution of an individual fiber is governed by its embedment length and orientation relative to the crack, as well as by mechanical anchorage, friction, and interfacial adhesion. Failure may occur through progressive pull-out, interfacial debonding, or fiber rupture. Pull-out can dissipate energy when bond and embedment permit gradual slip, whereas very weak contact may cause premature debonding and a fiber aligned nearly parallel to the crack may contribute little (Peled and Bentur, 2000; Sadrolodabaee et al., 2021a).

Studies of recycled PET fibers show that polymer fibers can improve crack control and aspects of tensile or flexural response when their geometry and incorporation are controlled (Foti, 2013; Fraternali et al., 2011; Ochi et al., 2007). These studies are useful for understanding polymer-fiber mechanisms, but their fibers were manufactured or cut from comparatively controlled PET sources. They do not represent a mixed wastewater-derived RTF stream.

Textile-waste studies introduce additional variability. Carpet fibers, production fabrics, and blended fabric waste differ in polymer, length, surface texture, and preparation, and reported performance changes accordingly (Idrees et al., 2023; Tran et al., 2023; Wang, 1999). Wastewater-derived RTF adds further uncertainty through mixed composition, residual contaminants, entanglement, and broad geometry. Mechanisms established for controlled fibers should therefore be treated as hypotheses to be tested, not as proof of RTF performance.

2.3.2 Fresh-State Behavior and Dispersion

Textile-derived fibers frequently reduce mortar or concrete flowability by increasing internal friction, physically obstructing particle movement, and retaining water or paste at their surfaces. The magnitude depends on fiber content, aspect ratio, flexibility, surface condition, and mixing sequence. Experimental and review studies consistently identify fresh-state handling and dispersion as major constraints, although the response varies with the fiber and matrix (Jayalath et al., 2024; Sasi et al., 2024; Tran et al., 2023).

Increasing fiber content raises the probability of fiber–fiber contact, entanglement, and agglomeration. Clusters can trap air, prevent complete mortar penetration, and produce fiber-rich regions beside fiber-poor regions. These defects may increase specimen variability and offset crack-bridging benefits. Evidence from carpet and textile-waste concrete also shows that dosage effects are not monotonic; the best-performing content is specific to the feedstock and mixture rather than transferable as a universal optimum (Idrees et al., 2023; Jayalath et al., 2024).

Mixing sequence and energy influence dispersion. Gradual addition can help separate flexible fibers, while rapid introduction can promote balling. Excessive mixing may also damage or re-entangle some waste fibers. Because geometry and moisture condition differ among studies, a procedure effective for one processed textile fiber may not be suitable for another (Rahman et al., 2022; Tran et al., 2022).

2.3.3 Flexural and Compressive Performance

Fiber effects are often more apparent under tension or bending than under uniaxial compression because crack bridging acts directly across opening cracks. Adequately distributed fibers may improve crack control, toughness, residual load transfer, or flexural strength. Peak strength, however, is not guaranteed to increase; poorly bonded or unfavorably oriented fibers may add little, and defects created during incorporation can dominate the response (Rahman et al., 2022; Sasi et al., 2024; Tran et al., 2022).

Compressive results are more variable. Fibers can restrain localized cracking, but clusters, entrapped air, weak interfaces, and reduced matrix continuity can lower the effective load-bearing area. Studies of recycled textile, carpet, and fabric fibers report outcomes that depend on fiber content, source, geometry, and mixture design rather than one consistent increase or decrease (Idrees et al., 2023; Jayalath et al., 2024; Tran et al., 2023).

This variation explains why results from different feedstocks cannot be compared by dosage alone. A mass percentage of long, low-density, flexible fibers does not create the same number of fibers, surface area, or spatial network as the same mass percentage of short, dense, or stiff fibers. Matrix composition, water-to-binder ratio, specimen geometry, curing, and test method introduce further differences. No conversion from mass fraction to volume fraction is justified without verified constituent densities and a defined calculation.

The three Sadrolodabaee studies (2021) illustrate the importance of reinforcement form. Short textile-waste fibers, nonwoven fabrics, and multilayer laminates produced different flexural and durability responses because their continuity and placement differed (Sadrolodabaee et al., 2021a, 2021b, 2021c). These systems provide a useful comparison for architecture, but their engineered nonwovens and relatively high fiber contents are not equivalent to a loose central RTF layer under the nominal 1 wt% experimental designation.

2.3.4 Durability and Fiber–Matrix Interaction

Long-term performance depends on moisture transport, matrix porosity, fiber stability, and the evolution of the fiber–matrix interface. Polymer type is important: PET fibers have shown usable performance in alkaline cementitious environments in controlled studies, while smooth surfaces can limit adhesion (Ochi et al., 2007). Cellulose-containing textile fibers have different

water uptake and aging behavior, and mixed textile waste may combine several responses within one composite (Sasi et al., 2024; Tran et al., 2022).

Durability evidence for textile-waste cement composites is material- and configuration-specific. Sadrolodabaee et al. (2021b, 2021c) evaluated controlled nonwoven and short-fiber systems, but those results do not establish the durability of the mixed wastewater-recovered feedstock used here.

Fractured-surface microscopy can show fibers, gaps, cracks, or fiber-rich regions, but chemical bonding, hydration products, and interfacial chemistry require higher-resolution analytical methods. Preparation and fracture can themselves create discontinuities.

2.4 Influence of Fiber Dosage and Placement Configuration

Fiber content and spatial arrangement are related but distinct variables. Dosage controls the total fiber mass introduced, whereas configuration controls where that mass is located. At the same nominal dosage designation, mixing the fibers throughout the mortar is intended to produce a distributed fiber arrangement, while central layered placement deliberately creates a fiber-rich internal zone.

The literature does not support a universal optimum dosage for recovered or recycled textile fibers. Reported optima depend on feedstock, geometry, matrix, workability control, and the measured response. Increasing dosage may provide more potential crack bridges, but it also increases surface area, fiber interaction, and the risk of poor compaction (Idrees et al., 2023; Sadrolodabaee et al., 2021c; Sasi et al., 2024).

2.4.1 Fibers Incorporated through Mixing

Randomly dispersed short fibers can intersect cracks at multiple locations and orientations throughout a specimen. Their effectiveness depends on the probability that fibers cross a developing crack with sufficient embedment. Random distribution is therefore not synonymous with effective dispersion: a mixture can be random at the specimen scale while still containing clusters and fiber-free regions (Sasi et al., 2024; Tran et al., 2022).

Experimental studies using carpet fibers, textile waste, and fabric-derived fibers show that mixing procedure and fiber geometry influence both workability and mechanical response (Idrees et al., 2023; Jayalath et al., 2024; Tran et al., 2023; Wang, 1999). Differences among these studies also show why a result obtained with cut or mechanically processed fibers should not be assumed for flexible, entangled wastewater-derived RTF.

Homogeneous mixing has a potential advantage under compression because it avoids a deliberately continuous fiber-rich plane. This advantage is conditional: dispersed clusters or

entrapped air can still interrupt the matrix and lower strength. Under bending, only the fraction of fibers favorably located and oriented relative to the crack can contribute to bridging.

2.4.2 Layered and Localized Placement

Engineered textile-reinforced mortar uses continuous fabrics or meshes positioned at defined depths, often near tensile zones. Fabric geometry, yarn continuity, impregnation, bond, and number of layers govern the composite response (Koutas et al., 2019; Peled and Bentur, 2000). These systems can mobilize reinforcement efficiently because their architecture is controlled.

Nonwoven textile-waste layers provide a closer comparison to recycled fibers, but they remain manufactured sheets with defined continuity and thickness. Studies comparing short random fibers with textile or nonwoven reinforcement show that architecture and layer number strongly influence flexural behavior (Sadrolodabaee et al., 2021a, 2021b). Their results cannot be transferred directly to loose RTF placed manually between mortar lifts.

A loose fiber layer can increase local fiber availability, but it can also impede mortar penetration and compaction. Its behavior depends on layer depth, thickness, continuity, local fiber concentration, and bonding to the surrounding mortar. Under compression, a poorly integrated fiber-rich zone may act as a discontinuity; under bending, its contribution depends on whether the crack path intersects the layer and whether the fibers are adequately embedded.

2.4.3 Relevance to Wastewater-Derived RTF

Wastewater-recovered RTF differ from most reinforcing materials reviewed above. The same material batch used here had previously been characterized by micro-FTIR and contained acrylic, polyester, polypropylene, polyamide, cotton, viscose, and wool (Akyıldız et al., 2025b). Its geometry was not standardized before mixing and residual processing substances may remain.

For this feedstock, placement may be as influential as total mass. Homogeneous mixing distributes the opportunity for crack intersection but requires effective separation of irregular fibers. Central layered placement avoids dispersing fibers through the full volume but creates a high local concentration whose integration with the adjacent mortar is uncertain.

These configurations may affect flexure and compression differently. A developing flexural crack may encounter either a distributed fiber population or a concentrated central zone. Compressive loading, in contrast, relies strongly on continuous load transfer through the matrix and may be more sensitive to a poorly compacted internal region. These are testable expectations derived from the literature, not findings assumed in advance.

Within the literature set reviewed here, no primary study was identified that directly compared mixed incorporation and internal layered placement of loose wastewater-recovered textile fibers at the same dosage in cementitious mortar. Existing evidence concerns industrial

microfiber occurrence and reuse, randomly dispersed solid-textile-waste fibers, controlled nonwoven layers, or engineered textile reinforcement. A direct experiment is therefore required before the behavior of the present RTF configurations can be inferred.

2.5 Research Gap and Positioning of the Present Study

The literature establishes that textile-processing wastewater is a measurable fiber source; treatment can transfer fibers to solids rather than destroy them; wastewater-derived fibrous material has been valorized in acoustic panels; and other textile wastes have been incorporated into cementitious materials (Akyıldız et al., 2022; Akyıldız et al., 2025a, 2025b; Malchiodi et al., 2022; Rahman et al., 2022).

What remains uncertain is the transferability of that cementitious evidence to wastewater-derived RTF. Most construction studies use cut fabrics, carpets, garments, production residues, controlled polymer fibers, or engineered nonwoven sheets. Those materials differ from the present feedstock in composition control, geometry, cleanliness, continuity, and preparation. The observed behavior of commercial or mechanically recycled fibers cannot therefore establish the behavior of a heterogeneous wastewater-derived stream.

A second uncertainty concerns configuration. Random short-fiber reinforcement and engineered layered reinforcement have both been studied, and direct comparisons confirm that architecture matters (Sadrolodabaee et al., 2021a). However, no primary study was identified in the literature reviewed for this thesis that directly compared mixed incorporation and internal layered placement of loose wastewater-recovered textile fibers at the same dosage in cementitious mortar.

The present study addresses this narrow gap through Control, Mixed 1% RTF, and Layered 1% RTF mortar groups. Parent prisms were tested in three-point flexure and paired half-prisms in compression. Selected surfaces were examined qualitatively using a HIROX digital microscope to compare visible features.

The contribution is preliminary and configuration focused. It does not establish a polymer-specific mechanism, optimize dosage, or demonstrate a structural application.

Standardized fresh-state testing, durability, direct characterization of future material batches, SEM/EDS interface analysis, and life-cycle assessment remain outside the scope. The same-batch micro-FTIR evidence used here should not be confused with a micro-FTIR analysis performed as part of the present thesis.

3. Materials

3.1 Recovered Textile Fibers

3.1.1 Source, Recovery, and General Description

The RTF originated from wastewater generated during a fabric-raising process using a Biancalani machine at a textile company in Türkiye. The wastewater was sampled directly after raising and before the stream joined the main treatment-plant influent. These source and recovery operations preceded this thesis experiment. Figure 3.1 shows the recovered material under ultraviolet light.



Figure 3.1. Recovered textile fibers under ultraviolet-light microscopy. The response is qualitative and does not establish chemical identity; no readable scale overlay was present in the supplied source image.

According to the project documentation, the wastewater was filtered on site using approximately 0.7 µm-pore, 47 mm glass-fiber filters (Whatman). The retained material was stored in a plastic container, resuspended in distilled water, treated with 15% H_2O_2 at room temperature for five days, washed with ECE detergent, and rinsed (Akyıldız et al., 2023). These prior recovery and conditioning steps preceded the present mortar experimental campaign.

The same recovered material batch had previously been characterized by micro-FTIR in Akyıldız et al. (2025b), which identified acrylic, polyester, polypropylene, polyamide, cotton, viscose, and wool. Micro-FTIR was not repeated in this thesis. The feedstock was visibly heterogeneous in color, morphology, and length, and some individual fibers fluoresced under ultraviolet light; fluorescence was treated only as a qualitative observation.

3.2 Cement

Holcim CEM II/B-LL 42.5R cement was used as the binder in all groups.

3.3 Standard Sand

Standard sand was used as fine aggregate. The nominal reference proportions followed BS EN 196-1:2016, while the preparation procedure included departures described in Chapter 4.

3.4 Mixing Water

The laboratory record documents 225 g of nominal liquid water for the reference formulation.

3.5 Mortar Mix Design

The laboratory record documents a reference mortar formulation of 450 g cement, 1350 g standard sand, and 225 g liquid water, corresponding to a nominal w/c of 0.50 and a sand-to-cement mass ratio of 3.0. For the actual experiment, one common base-mortar batch was prepared and then allocated sequentially to the three specimen groups. The accessible records do not document the total scale of that common batch or the mass of mortar allocated to each group; therefore, group-wise cement mass and effective RTF wt% cannot be independently reconstructed.

The RTF-containing groups were designated nominal 1 wt% RTF according to the experimental plan.

The laboratory record contains a 4.5 g calculation for a nominal 1 wt% target relative to the reference 450 g cement quantity; it does not establish that 4.5 g was applied separately to each sequentially allocated RTF group. Control specimens contained no RTF. Because the common mortar batch was split sequentially and the subgroup mortar masses were not recorded, the exact realized RTF mass fraction in the Layered and Mixed portions cannot be independently reconstructed from the available documentation.

Table 3.1. Common-batch allocation and nominal RTF incorporation.

Group	Base mortar source	RTF information	Incorporation and casting order
Control	Common parent mortar batch	0 g	Cast first; no RTF
Layered	Same common batch	Nominal 1 wt% designation; exact group allocation unverified	Loose fiber-rich region between lifts; cast second
Mixed	Remaining common batch	Nominal 1 wt% designation; exact group allocation unverified	RTF mixed into remaining mortar; cast last

Note. The reference mortar proportion used in the experiment consisted of 450 g cement, 1350 g standard sand, and 225 g water. No ice was used during the actual mortar preparation. The experiment used one common mortar batch for all groups, and the exact mortar mass allocated to each subsequent configuration was not recorded. The 4.5 g value is therefore retained only as the nominal 1 wt% calculation relative to the reference cement mass; the exact group-wise RTF mass fraction cannot be independently reconstructed.

3.6 Specimen Groups and Identification

Nine prisms were prepared, with three specimens assigned to each of the Control, Layered, and Mixed groups. All nine prisms originated from one common base-mortar batch and therefore do not constitute independent mortar-batch replicates.

The groups were produced sequentially from the common mortar batch. Control prisms were cast first without RTF. For the Layered group, a subsequent portion of mortar was placed in lifts, and loose RTF was introduced in a local intermediate region. RTF was then incorporated into the remaining mortar before the Mixed prisms were cast. ‘Mixed’ describes the incorporation method and does not imply quantitatively verified homogeneity. The exact Layered-zone thickness, continuity, fiber allocation, and orientation relative to loading were not documented.

The groups and specimen identifiers are summarized in Table 3.2.

Table 3.2. Specimen groups used in the experimental program.

Specimen IDs	Group	RTF designation	Placement	Batching / specimen structure
1–3	Layered	Nominal 1 wt% label	Loose localized internal region	3 prism specimens; shared common mortar batch; cast second
4–6	Mixed	Nominal 1 wt% label	Added during mixing	3 prism specimens; shared common mortar batch; cast last
7–9	Control	0 wt%	No RTF	3 prism specimens; shared common mortar batch; cast first

4. Experimental Methods

4.1 Experimental Program and Chronology

The program comprised fiber characterization, preparation of three mortar groups, flexural testing of parent prisms, qualitative digital-microscope observation, and compression testing of paired half-prisms. Table 4.1 distinguishes the initial 28-day testing plan from the actual dates and ages.

Table 4.1. Documented experimental chronology.

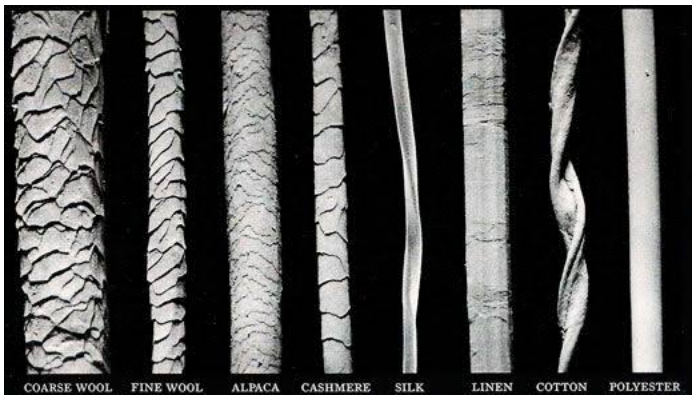
Activity	Documented date/age	Status
Mortar casting	16 February 2026 (day 0)	Recorded
Demolding	Approximately 24 h after casting	Recorded; exact clock time not supplied
Water curing	Documented to approximately day 28	Post-curing storage conditions not documented
Initial mechanical-test plan	28 days	Planned, not the actual test age
Flexural testing	13 April 2026 (56 days)	Recorded
Digital-microscope observation	22 May 2026 (95 days)	Recorded
Compression testing	12 June 2026 (116 days)	Date verified from the embedded test pert II record

4.2 Characterization of Recovered Textile Fibers

Before incorporation, 100 randomly selected fibers were examined using optical and ultraviolet-light microscopy to describe color, fluorescence response, visual morphology, and length. These observations did not provide chemical identification. Representative fields are shown in Figures 4.1 and 4.2.

Color was recorded visually. Ultraviolet-light response was classified as no visible fluorescence or blue fluorescence. Fluorescence was treated only as a qualitative indicator because dyes, optical brighteners, and finishing agents may contribute to the response.

Visual morphology was classified as synthetic-like or natural-like. Smoother, more regular fibers of relatively consistent thickness were recorded as synthetic-like; more irregular fibers with variable surface texture or thickness were recorded as natural-like. These categories were not equated with polymer proportions.



The same material batch had previously been characterized by micro-FTIR in Akyıldız et al. (2025b). That prior result provides batch-level supporting evidence, but the individual fibers visually classified here was not analyzed one by one by spectroscopy.

Length was measured from microscope images for the 100 selected fibers. Minimum, maximum, mean, median, sample standard deviation, quartiles, and interquartile range were calculated. The complete raw 100-value dataset was not available in the accessible project files for reconstruction of a histogram.

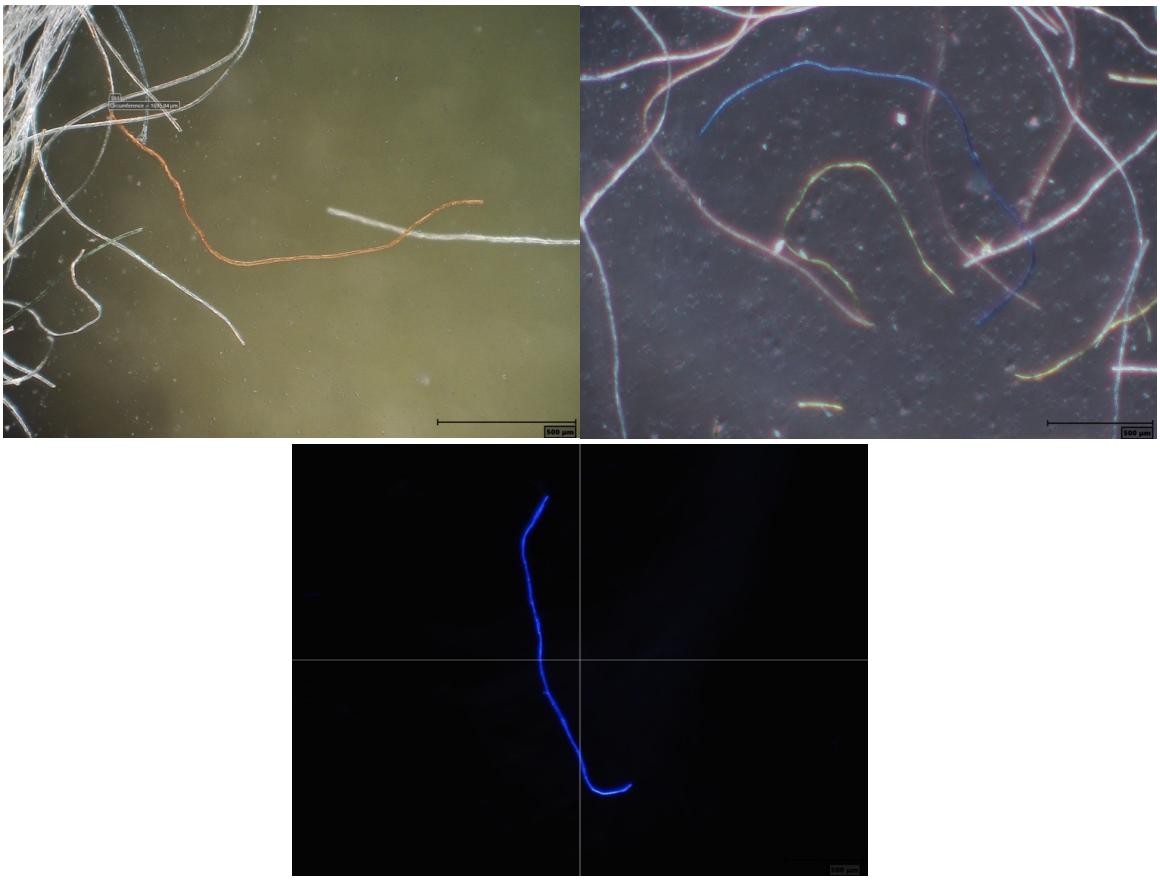


Figure 4.1. Representative optical and ultraviolet-light images of recovered textile fibers; the visible scale bars are 500 µm.

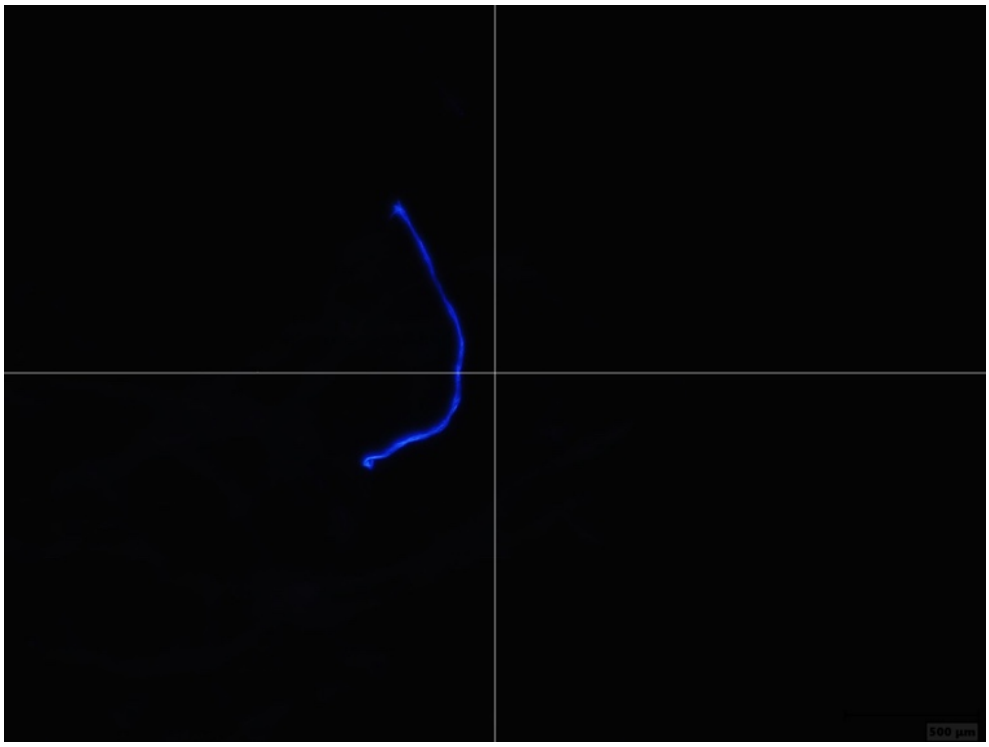


Figure 4.2. Additional ultraviolet-light image of a recovered textile fiber; the visible scale bar is 500 µm.

4.3 Preparation of Mortar Specimens

Mortar preparation was carried out on 16 February 2026. The original plan was mechanical testing at 28 days; actual test ages are reported in Table 4.1.

A common base mortar was prepared for the full casting sequence. Control prisms were filled first from the fiber-free mortar. A second portion was then used for the Layered prisms, where loose RTF was placed between mortar lifts. RTF was subsequently mixed into the remaining mortar, which was used to cast the Mixed prisms last. The nominal reference formulation and RTF target recorded in the laboratory documentation are summarized in Table 3.1. Polystyrene molds were labeled for the Control, Mixed, and Layered groups (Figure 4.3).

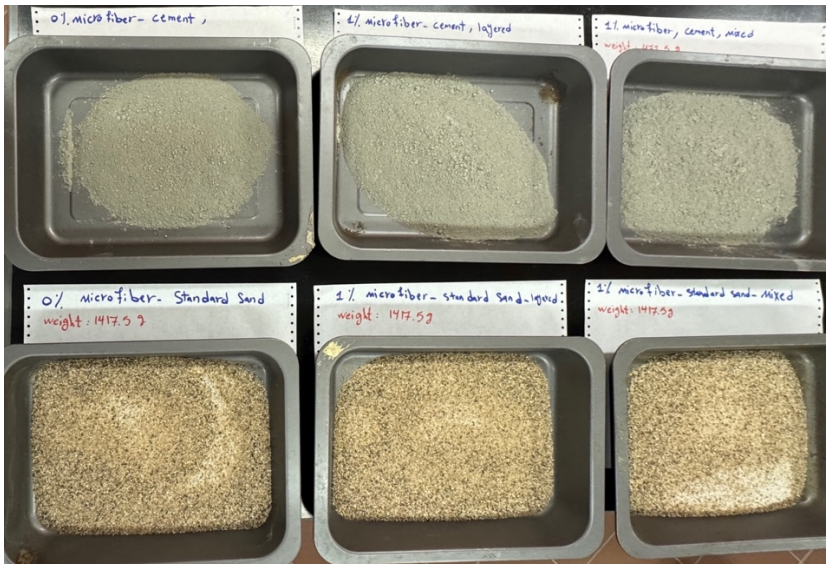


Figure 4.3. Preparation and weighing of mortar constituents before mixing.

4.4 Mixing Procedure

A handheld electric paddle mixer was used because the available laboratory mortar mixer was not suitable for the batch size. Exact mixer speed, mixing duration, and mixing energy were not documented and are therefore not reconstructed. The mixer is shown in Figure 4.4.

The common base mortar was initially mixed without RTF. Control prisms were cast from the first allocated portion. For the Layered specimens, loose RTF was placed between mortar lifts in the next allocated portion. RTF was then introduced gradually into the remaining mortar and manually encouraged to disperse before the Mixed prisms were cast; no quantitative distribution measurement was performed (Figure 4.5).

For the Layered specimens, the fiber-rich region was positioned nominally near mid-depth between successive mortar lifts. The exact layer thickness, continuity, fiber allocation, and orientation relative to flexural and compression loading were not recorded.



Figure 4.4. Mortar mixing with a handheld electric paddle mixer.



Figure 4.5. Incorporation of recovered textile fibers during mortar preparation.

4.5 Casting and Compaction

Fresh mortar was placed in 40 × 40 × 160 mm polystyrene molds. Casting and manual compaction were performed cautiously because the molds were relatively compliant. Compaction energy was not quantified.

Upper surfaces were leveled manually, and specimens were labeled by group and identifier (Figure 4.6).

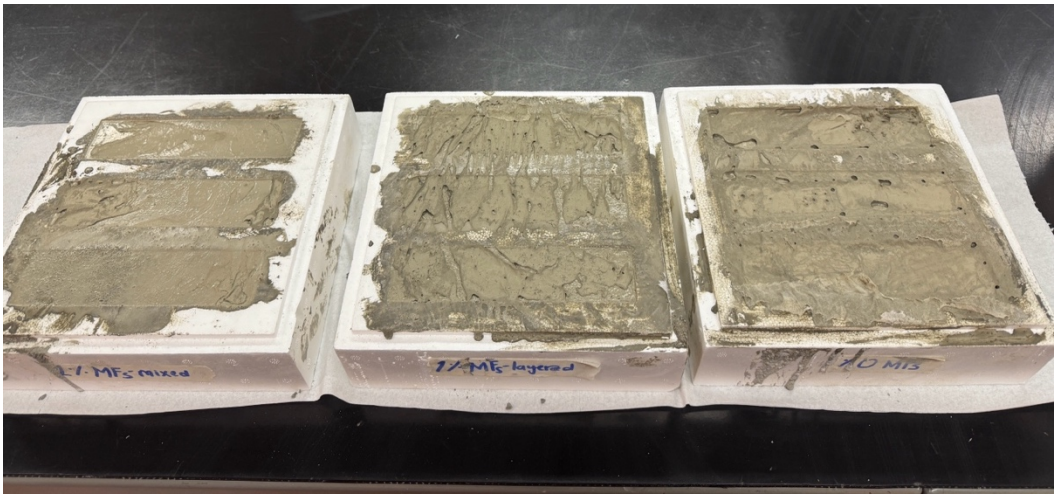


Figure 4.6. Cast mortar prisms in 40 × 40 × 160 mm polystyrene molds.

4.6 Demolding and Curing

Specimens were demolded after approximately 24 h and submerged in water until approximately 28 days. The available records do not establish the storage conditions between the end of this documented water-curing period and the later tests. Figure 4.7 documents the water-curing stage.

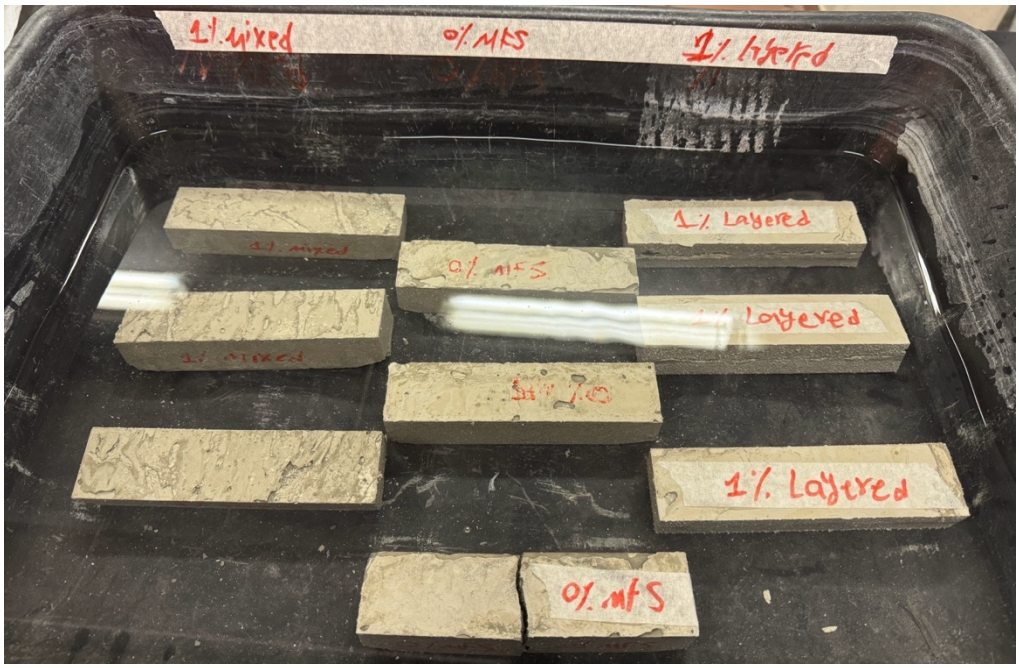


Figure 4.7. Water curing of demolded mortar prisms.

4.7 Mechanical Testing Sequence and Actual Ages

The initial plan was to test at 28 days. In practice, full prisms were tested in flexure at 56 days; the resulting halves were later tested in compression at 116 days. Three flexural values were intended per group, and six compression values were obtained. The three prisms within each group were specimens drawn from the same common mortar batch rather than independent batch replicates; additionally, each A/B compression pair originated from one parent prism.

4.8 Flexural Strength Test

Flexural testing used a three-point configuration with reference to BS EN 196-1:2016 (BSI, 2016). The full experimental program should not be described as fully standard-compliant because mixing, molding, compaction, and timing differed from the standard procedure. The support span was 100 mm, and testing took place on 13 April 2026 (56 days).

The fixture and support-span verification are shown in Figure 4.8.

A MATEST Unitronic frame fitted with a 50 kN load cell was used. The applied loading rate and calibration record were not available in the accessible documentation.

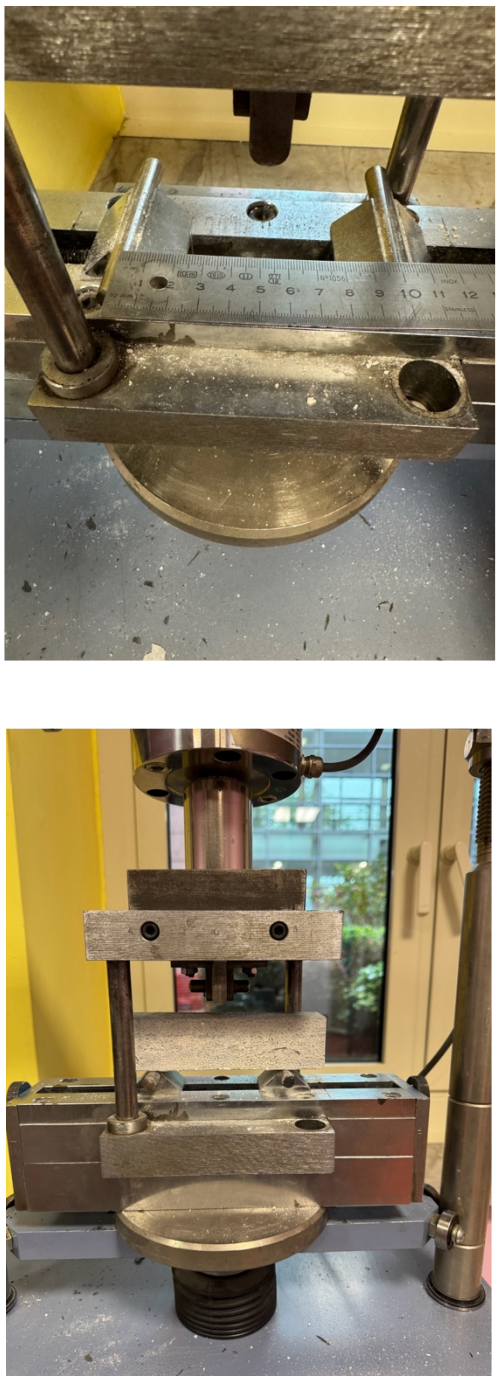


Figure 4.8. Mortar prism in the three-point flexural fixture and verification of the 100 mm support span.

Flexural strength was calculated from the recorded maximum load and the measured specimen width and depth:

$$R_f = 1.5\, F_f\, l \,/\, (b\, d^2)$$

where R_f is flexural strength (MPa), F_f is maximum flexural load (N), l is supporting span (mm), b is measured specimen width (mm), and d is measured specimen depth at the section (mm).

Measured dimensions were used in place of an assumed 40 × 40 mm square section.

4.9 Compressive Strength Test

Compression testing was performed on 12 June 2026 (116 days) on the A/B half-prisms produced by the earlier flexural tests. Each identifier retained its parent-prism number and an A or B suffix.

Each half-prism was centered in the compression fixture. The load was applied to the nominal 40 × 40 mm end area (A = 1600 mm²) until failure, and the maximum load was recorded. The exact loading rate was not documented.

Compressive strength was recalculated from the measured maximum load using:

$$R_c = F_c \,/\, A$$

where R_c is compressive strength (MPa), F_c is maximum compressive load (N), and A is the loaded area (1600 mm²).

For loads reported in kN and A = 1600 mm², the equivalent expression is:

$$R_c = 0.625\, F_c \quad \text{(for } F_c \text{ in kN)}$$

The software screen displayed an automatic stress based on a different area setting; those values were not used. Table 5.7 reports strengths recalculated from peak load using the 40 × 40 mm area.

Six values were obtained per group from three parent prisms. Group means and sample standard deviations are descriptive. The parent prisms were produced from one common mortar batch, and each A/B pair came from one parent prism; the six half-prism measurements therefore must not be treated as independent experimental units.

The compression system was a Zwick/Roell installation operated with testXpert II software. The exact frame model, calibration record, and loading rate were not supplied in the accessible documentation. Figures 4.9–4.11 document the system and fixtures.



Figure 4.9. Zwick/Roell compression testing system used for the mortar half-prisms.



Figure 4.10. Compression fixture used for the mortar half-prisms.



Figure 4.11. Mortar half-prism centered in the compression fixture before loading.

4.10 Digital-Microscope Observation of Mortar Specimens

Selected fractured and cut mortar surfaces were examined on 22 May 2026 (95 days) using a HIROX digital microscope. The Control, Layered, and Mixed groups were compared qualitatively.

Observation focused on visible fiber-like elements, fiber-rich regions, matrix texture, aggregate, cracks, local discontinuities, and dark or void-like features. Features in Control specimens provided a baseline, so dark regions in RTF-containing specimens were not automatically attributed to fibers or fiber-induced voids.

These selected two-dimensional fields cannot determine chemical identity, quantitative porosity, bond strength, interfacial chemistry, or three-dimensional distribution and orientation. They provide qualitative context only.

5. Results

5.1 Characterization Results of Recovered Textile Fibers

The 100-fiber visual dataset is summarized in Figure 5.1 and Tables 5.1–5.4. It describes color, fluorescence, visual morphology, and length; it does not quantify polymer composition.

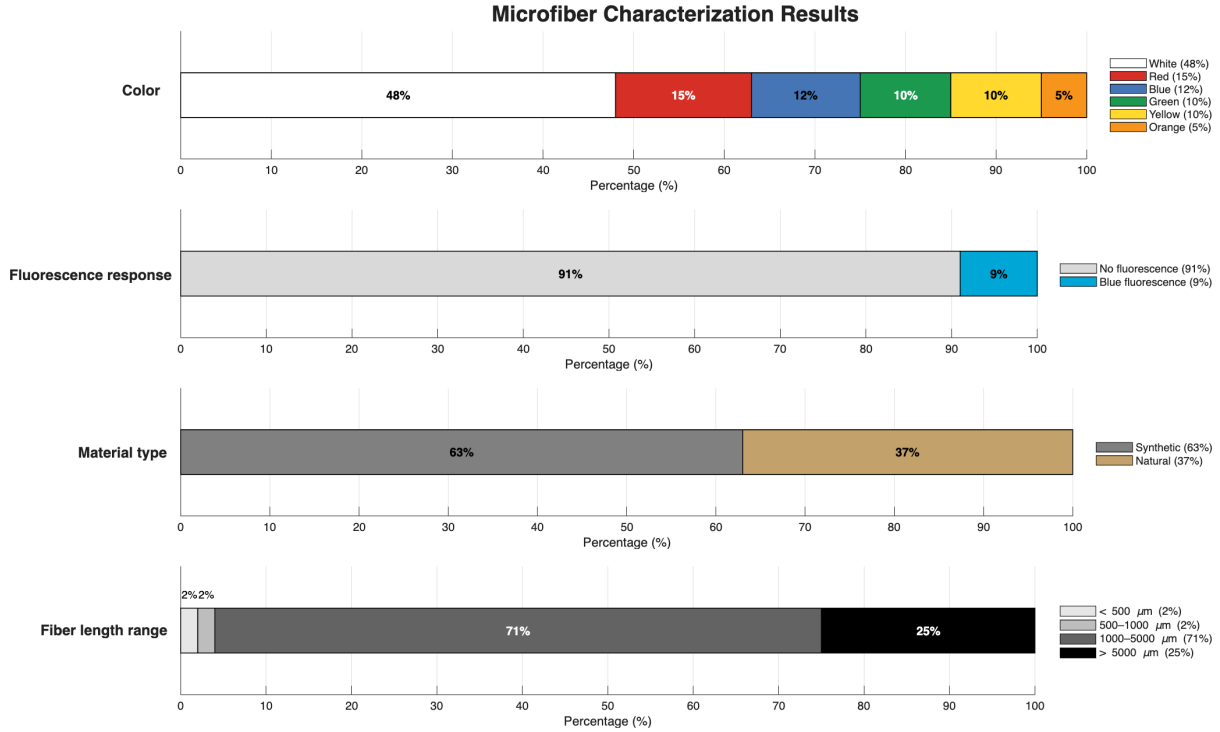


Figure 5.1. Summary of the 100-fiber visual characterization dataset.

5.1.1 Color Distribution

Table 5.1. Color distribution of the 100 selected recovered textile fibers.

Color	Number of selected fibers	**Percentage (%)**
White	48	48
Red	15	15
Blue	12	12
Green	10	10
Yellow	10	10
Orange	5	5
Total	100	100

White was the most frequent observed color (48%), followed by red (15%), blue (12%), green and yellow (10% each), and orange (5%).

The variation confirms visual heterogeneity. Color alone does not establish polymer or source because dyes and finishing processes can produce different colors in the same fiber family.

5.1.2 Fluorescence Response

Table 5.2. Ultraviolet-light fluorescence response of the 100 selected fibers.

Fluorescence response	Number of selected fibers	**Percentage (%)**
No fluorescence	91	91
Blue fluorescence	9	9
Total	100	100

Ninety-one fibers showed no visible fluorescence and nine showed blue fluorescence.

Blue fluorescence may reflect dyes, optical brighteners, or finishing agents, but cannot provide chemical identification.

5.1.3 Apparent Material Type Distribution

Table 5.3. Visual morphology categories assigned to the 100 selected fibers.

Apparent material type	Number of selected fibers	Percentage (%)
Synthetic-like	63	63
Natural-like	37	37
Total	100	100

Visual morphology classified 63 fibers as synthetic-like and 37 as natural-like. The labels describe appearance only.

Synthetic-like fibers generally appeared smoother and more regular, with comparatively consistent thickness; natural-like fibers appeared more irregular in morphology, texture, or thickness. The classification was not validated against a chemically labeled reference set.

The same material batch had previously been characterized by micro-FTIR in Akyıldız et al. (2025b), identifying acrylic, polyester, polypropylene, polyamide, cotton, viscose, and wool. Because the visually classified individual fibers were not analyzed one by one, 63% and 37% are not polymer-composition percentages.

No mechanical response is attributed to a specific polymer type on the basis of this visual classification.

5.1.4 Fiber Length Distribution

Table 5.4. Descriptive statistics for the 100 measured fiber lengths.

Statistic	Value
Number of fibers measured	100
Minimum length	0.255 mm
Maximum length	19.333 mm
Mean length	4.229 mm
Standard deviation	3.815 mm

Statistic	Value
Median length	2.544 mm
First quartile, Q1	2.304 mm
Third quartile, Q3	4.869 mm
Interquartile range	2.565 mm

Lengths ranged from 0.255 to 19.333 mm, demonstrating a broad distribution.

The mean was 4.229 mm, the median 2.544 mm, and the sample standard deviation 3.815 mm. The mean above the median is consistent with a right-skewed distribution influenced by longer fibers.

5.1.5 Microscopic Appearance of Recovered Textile Fibers

Representative fields showed fibers of different colors, lengths, shapes, and degrees of entanglement. Both isolated fibers and tangled clusters were visible; Figure 5.3 provides an example length measurement.

Surface appearance ranged from relatively smooth and regular to irregular and variable in thickness, consistent with the visual categories in Section 5.1.3.

These images document morphology and fluorescence only; they do not identify individual polymers.

The observed physical heterogeneity is relevant when interpreting handling and specimen variability, but no causal mechanical mechanism was measured.

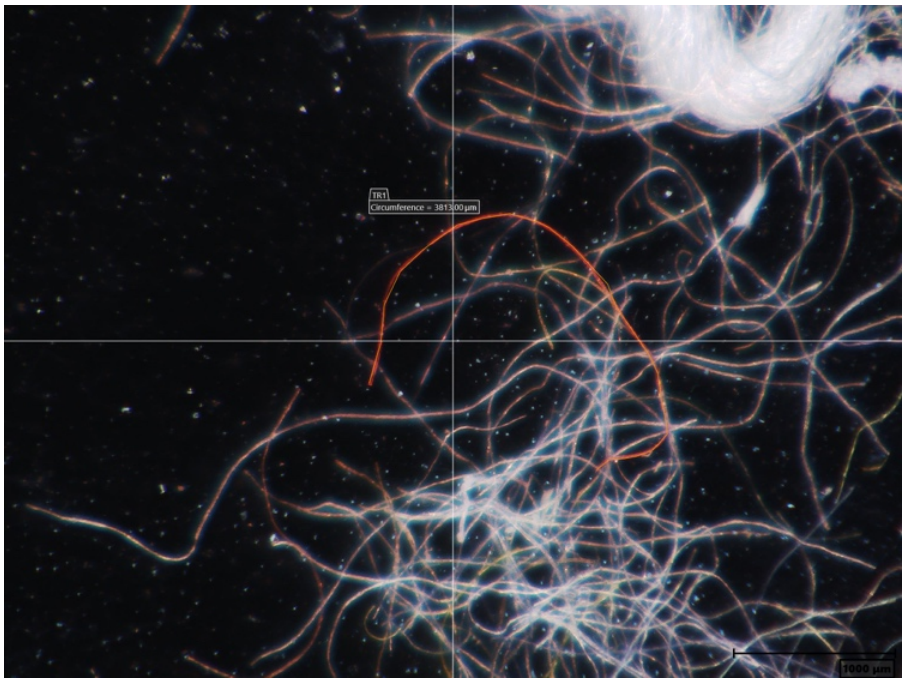


Figure 5.3. Example fiber-length measurement; the image retains its original measurement overlay and 1000 µm scale bar.

5.2 Qualitative Handling Observations

The Mixed mortar required continued manual attention during incorporation because visible entanglement and local clustering occurred.

The Layered method localized the loose fibers between mortar lifts but created an intentionally concentrated region whose geometry was not quantified.

Manual finishing left some surface irregularities. No standardized flow, fresh density, air-content, or temperature results were generated; the observations are qualitative only.

5.3 Flexural Strength Results

Three-point flexural tests were performed at 56 days on Control, Mixed 1% RTF, and Layered 1% RTF parent prisms. Raw results are reported in Table 5.5.

Only two Control results were valid because specimen 9 was damaged before a valid flexural test; its mean is therefore not a standard three-prism mean.

ID	Group	Test date	Width (mm)	Depth (mm)	Span (mm)	Length (mm)	F_f (N)	R_f (MPa)
1	Layered 1%	13/04/2026	40.63	41.79	100	160	3165	6.69
2	Layered 1%	13/04/2026	40.36	40.68	100	159	3653	8.20
3	Layered 1%	13/04/2026	39.77	41.29	100	159	3853	8.52
4	Mixed 1%	13/04/2026	39.92	40.51	100	160	3243	7.42
5	Mixed 1%	13/04/2026	40.47	40.29	100	160	3152	7.19
6	Mixed 1%	13/04/2026	39.49	40.76	100	160	3165	7.23
7	Control	13/04/2026	40.07	40.22	100	159	3526	8.15
8	Control	13/04/2026	38.21	41.1	100	160	2882	6.69
9	Control	13/04/2026	40.64	40.04	100	160	No valid test	—

Table 5.5. Flexural results calculated using measured width and depth.

Descriptive group means and sample standard deviations are summarized in Table 5.6 and Figure 5.4.

Mix type	Valid specimens	Average flexural strength (MPa)	Standard deviation (MPa)
Layered 1%	3	7.80	0.98
Mixed 1%	3	7.28	0.12
Control	2	7.42	1.03

Table 5.6. Descriptive flexural-strength summary.

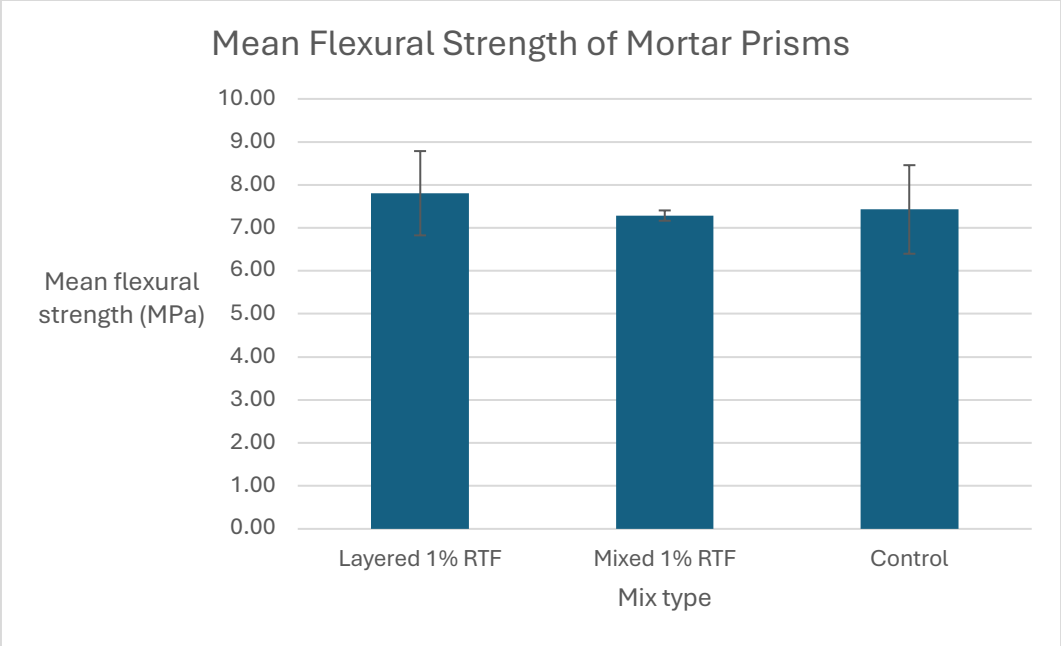


Figure 5.4. Descriptive mean flexural strength with sample standard-deviation error bars.

The descriptive means were 7.42 MPa for Control (n = 2), 7.28 MPa for Mixed (n = 3), and 7.80 MPa for Layered (n = 3). The differences were small. These n values are specimen counts, not independent mortar-batch replicates.

The Mixed values were closely grouped (SD 0.12 MPa), while Layered and Control were more variable. This does not demonstrate homogeneous three-dimensional distribution.

A supervisor record notes an improper failure mode for one Layered prism, but the specimen identifier is unavailable. All three recorded values are retained transparently; the Layered summary is therefore provisional.

5.4 Qualitative Digital-Microscope Observations

Selected fields from Control, Layered, and Mixed specimens were compared qualitatively for matrix texture, fiber-like elements, fiber-rich zones, cracks, discontinuities, and dark or void-like regions.

5.4.1 Reference Specimens

Control fields were matrix-dominated and contained aggregate, dark inclusions, and local discontinuities. Their presence shows that comparable dark regions in RTF-containing specimens cannot automatically be assigned to fibers or fiber-induced voids (Figure 5.5).

The Control fields provide a qualitative baseline only.

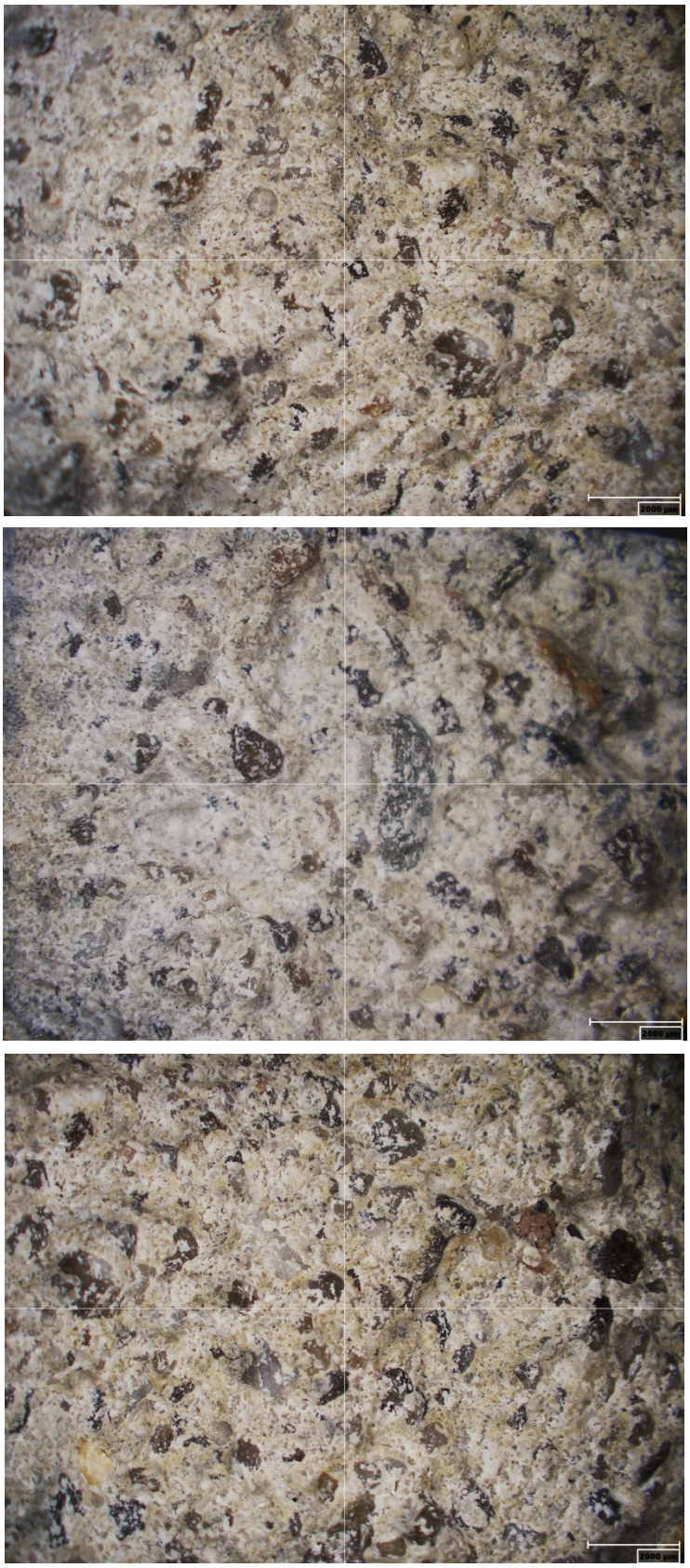


Figure 5.5. Reference-mortar fields without RTF. The retained source images show readable 2000 µm scale bars.

5.4.2 Layered 1% RTF Specimens

The observed Layered surfaces contained localized fiber-rich regions and visible boundaries with surrounding mortar, consistent with the placement method (Figure 5.6).

Local discontinuities and dark regions occurred near some fiber-rich zones. Possible explanations include incomplete matrix penetration, casting heterogeneity, fracture damage, or cutting artefacts; the images do not establish cause.

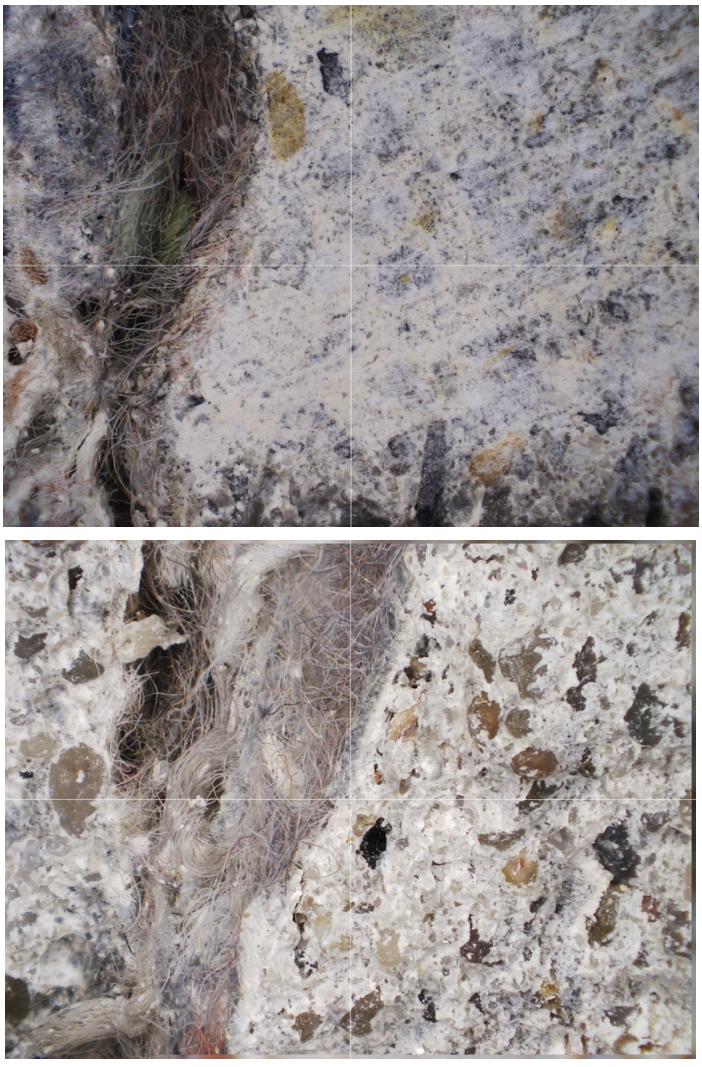




Figure 5.6. Layered 1% RTF fields showing localized loose-fiber regions. No readable scale overlay was present in the supplied source exports.

5.4.3 Mixed 1% RTF Specimens

Mixed fields were mainly matrix-dominated with dispersed fiber-like elements. No continuous fiber-rich layer was visible in the selected fields (Figure 5.7).

Local clusters, dark regions, and discontinuities remained visible. The selected fields do not prove complete or uniform three-dimensional distribution.

The observed surfaces were consistent with different placement patterns, but cannot quantify porosity, bond strength, interfacial chemistry, or causal failure mechanisms.

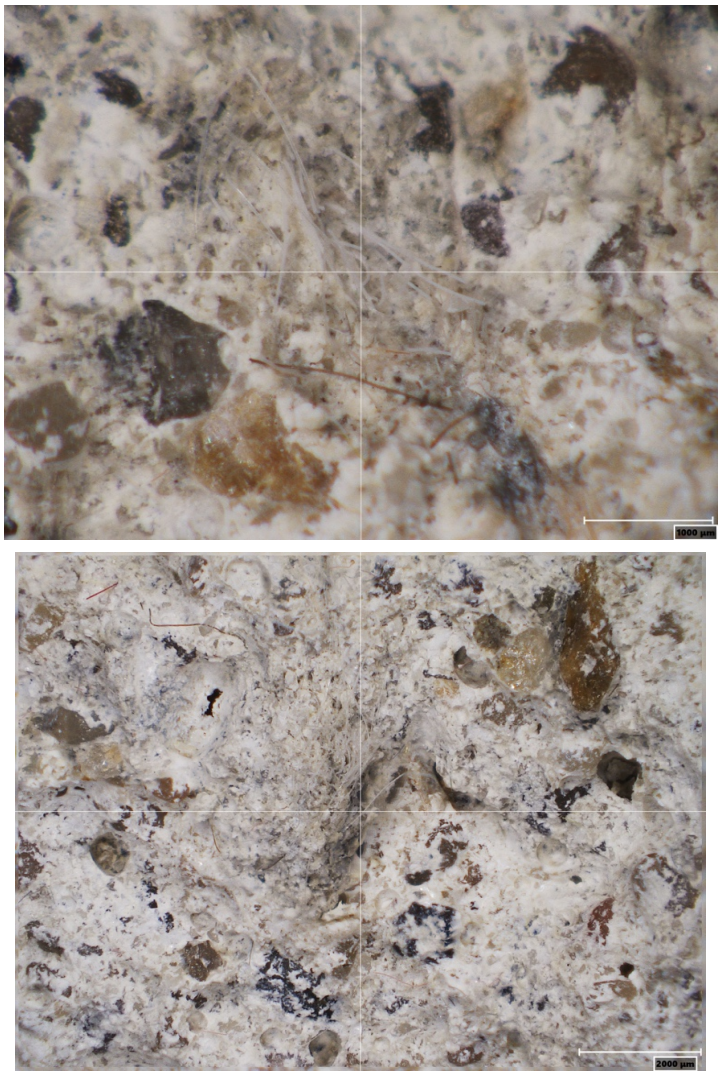


Figure 5.7. Mixed 1% RTF fields; retained source images show readable 1000 µm and 2000 µm scale bars.

5.5 Compressive Strength Results

Compression testing was performed at 116 days on paired A/B half-prisms from the flexural tests. IDs 1–3 were Layered, 4–6 Mixed, and 7–9 Control.

Eighteen half-prisms were tested. Strengths were recalculated from peak loads using A = 1600 mm². Table 5.7 retains every recorded result.

Each group's six measurements arose from three parent prisms produced from the same common mortar batch. A/B halves additionally share the same parent-prism history and are not independent experimental units.

5.5.1 Individual Compressive Strength Results

Peak loads and recalculated compressive strengths are presented in Table 5.7. Values ranged from 41.09 to 52.97 MPa for Layered, 52.24 to 60.85 MPa for Mixed, and 45.77 to 64.79 MPa for Control.

Table 5.7. Peak compression loads and strengths of paired mortar half-prisms.

Specimen ID	Mix group	Maximum load (kN)	Compressive strength (MPa)
1A	Layered 1%	68.55	42.84
1B	Layered 1%	75.25	47.03
2A	Layered 1%	84.75	52.97
2B	Layered 1%	74.69	46.68
3A	Layered 1%	65.74	41.09
3B	Layered 1%	80.58	50.36
4A	Mixed 1%	89.73	56.08
4B	Mixed 1%	92.84	58.02
5A	Mixed 1%	97.36	60.85
5B	Mixed 1%	93.69	58.56
6A	Mixed 1%	83.58	52.24
6B	Mixed 1%	92.71	57.94
7A	Control	103.66	64.79
7B	Control	92.41	57.75
8A	Control	74.39	46.49

Specimen ID	Mix group	Maximum load (kN)	Compressive strength (MPa)
8B	Control	73.23	45.77
9A	Control	90.39	56.49
9B	Control	101.76	63.60

Layered values were generally lower; Mixed values occupied a comparatively narrow range; Control showed the widest spread, including the paired low results from parent prism 8.

Although specimen 9 lacked a valid flexural value, half-prisms 9A and 9B remained suitable for compression and were retained.

5.5.2 Comparison of Mean Compressive Strength

Descriptive group means, sample standard deviations, and changes relative to Control are reported in Table 5.8 and Figure 5.8.

Table 5.8. Descriptive compression-strength summary.

Mix group	Tested half-prisms (parent prisms)	Mean compressive strength (MPa)	Standard deviation (MPa)	Change relative to control
Layered 1% RTF	6 (3)	46.83	4.45	−16.1%
Mixed 1% RTF	6 (3)	57.28	2.90	+2.6%
Control	6 (3)	55.82	8.16	Reference

The unfiltered means were 57.28 MPa for Mixed, 55.82 MPa for Control, and 46.83 MPa for Layered. Relative differences were +2.6% and −16.1%, respectively.

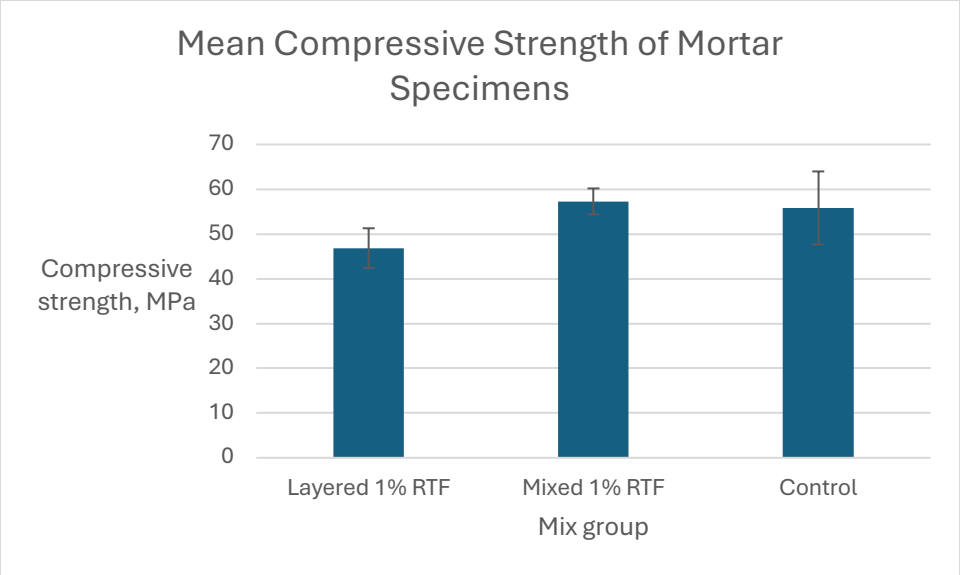


Figure 5.8. Descriptive mean compressive strength with sample standard-deviation error bars.

Mixed had the lowest sample standard deviation (2.90 MPa), followed by Layered (4.45 MPa) and Control (8.16 MPa).

The paired low Control values 8A and 8B came from one parent prism; their common history reinforces the need to acknowledge pairing.

The +2.6% Mixed–Control difference is a descriptive observation, not evidence of strengthening. Layered was descriptively lower under the conditions tested.

Applied only as a numerical screen, the BS EN 196-1:2016 ±10% individual-result evaluation criterion was satisfied by the Mixed set but not by the unfiltered Control or Layered sets. Because the full program departed from standard preparation and timing, this is not a claim of full standard compliance.

5.5.3 Failure Mode Observations

Post-compression visual inspection recorded local crushing, cracking, fragmentation, and separation. These observations were qualitative; a representative failure is shown in Figure 5.9.

Failure generally involved local crushing beneath the loaded area followed by cracks through the mortar body.

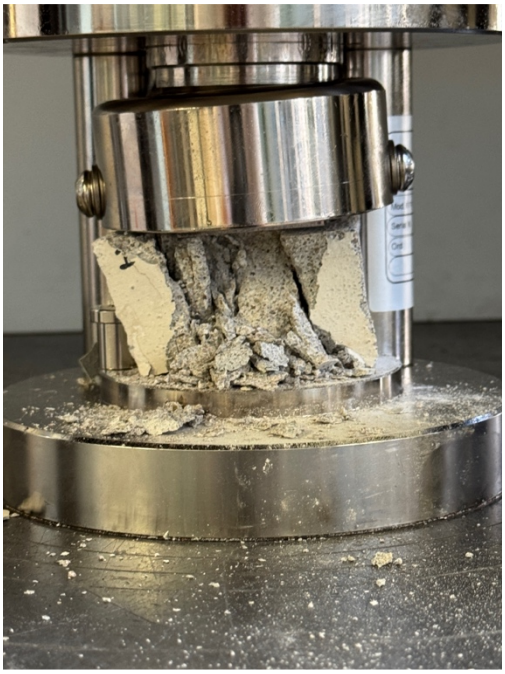


Figure 5.9. Representative local crushing of a mortar half-prism after compression.

Control specimens showed brittle matrix cracking and crushing; no fiber-related interpretation was made.

Mixed specimens also failed mainly by matrix crushing; their recorded peak strengths were more closely grouped.

Some Layered specimens showed separation near internal discontinuities. Visual inspection cannot establish whether fiber placement caused the lower mean (Figure 5.10).



Figure 5.10. Fractured mortar half-prism showing cracking, fragmentation, and separation after compression.

No failure image was used to infer bond strength, interfacial chemistry, or a causal mechanism.

6. Discussion

This preliminary experiment compared Mixed and Layered incorporation of wastewater-recovered RTF in mortar. Layered had the highest descriptive flexural mean but the lowest descriptive compression means; Mixed remained close to Control in flexure and had the highest unfiltered compression mean.

Interpretation is restricted by the use of one common mortar batch with sequential group allocation, three prism specimens per group, two valid Control flexural results, an unidentified improper Layered flexural failure, paired compression halves, departures from standard preparation, and qualitative microscopy. The discussion therefore concerns observed specimen-level trends and plausible explanations, not independently replicated or statistically established effects.

6.1 Feedstock Heterogeneity

The visual and dimensional dataset demonstrated a physically heterogeneous feedstock, including lengths both below and above the 5 mm operational microfiber threshold. The 63% synthetic-like and 37% natural-like categories describe morphology and are not chemical fractions.

This physical heterogeneity is consistent with textile-wastewater streams whose composition varies with processed textiles, operations, sampling point, and recovery method (Akyıldız et al., 2022; Akyıldız et al., 2025a; Ramasamy et al., 2022).

The same batch had previously been characterized by micro-FTIR and contained several synthetic, regenerated-cellulose, and natural fiber types (Akyıldız et al., 2025b). Micro-FTIR was not repeated here, and the prior batch-level result does not convert the visual categories into quantitative composition.

Broad length and visible entanglement may influence dispersion and crack intersection, as suggested by wider fiber-reinforced-cement literature, but orientation, interface quality, and crack bridging were not measured in this study.

6.2 Handling and Incorporation

The need for gradual RTF addition and manual attention during preparation of the Mixed portion is consistent with reported entanglement and clustering of irregular textile-derived fibers (Idrees et al., 2023; Sasi et al., 2024; Tran et al., 2022).

No flow, fresh-density, or air-content tests were performed, so fresh-state effects cannot be quantified.

Layered placement localized the fibers but introduced a concentrated region; Mixed placement aimed at distribution but did not demonstrate three-dimensional homogeneity. Because Control, Layered, and Mixed specimens were cast sequentially from one common batch, group configuration is also confounded with casting order and elapsed handling time. Undocumented mixing parameters, manual compaction, polystyrene molds.

6.3 Flexural Response

The small differences among descriptive flexural means do not establish strengthening. The Control mean used only two values and the Layered mean remains provisional because the improperly failed Layered specimen was not identified.

A local fiber-rich region could intersect a flexural crack, but loose RTF is not equivalent to an engineered mesh or nonwoven textile. Without load–deflection, crack-width, toughness, or residual-strength data, crack bridging and post-cracking benefit were not demonstrated (Koutas et al., 2019; Sadrolodabaee et al., 2021a, 2021b).

The close Mixed peak values show only low dispersion among the three recorded specimen results; they do not prove homogeneous fiber distribution or reproducibility across independently prepared mortar batches.

6.4 Digital-Microscope Observations

Selected two-dimensional fields were consistent with localized fiber-rich regions in Layered specimens and more dispersed fiber-like elements in Mixed specimens.

Dark regions and discontinuities also occurred in Control fields, so not every dark feature in RTF-containing mortar can be attributed to a fiber or fiber-induced pore.

Visible boundaries may reflect matrix penetration, casting heterogeneity, fracture, cutting, or surface preparation. The images cannot distinguish pull-out, debonding, rupture, quantitative porosity, or interfacial chemistry.

Microscopy therefore supplies qualitative context, not causal proof.

6.5 Compressive Response

The Mixed mean was descriptively 2.6% above Control and Layered 16.1% below Control. The small Mixed–Control difference is not evidence of strengthening.

The Mixed set passed the numerical ±10% individual-result evaluation criterion, whereas the unfiltered Control and Layered sets did not. These comparisons are exploratory because the full preparation and timing did not satisfy all BS EN 196-1:2016 requirements.

A concentrated discontinuity, incomplete matrix penetration, layer geometry, or compaction could plausibly contribute to the lower Layered values; comparable factors could influence flexure as well as compression. None was isolated experimentally.

The six half-prism values per group represent three A/B pairs from three parent prisms, all originating from the same common mortar batch; they are not six independent experimental units.

6.6 Combined Interpretation

Taken together, the mechanical data and selected microscope fields show an association between incorporation method and the observed responses under the tested conditions.

Mixed provided the more balanced descriptive response of the two RTF configurations. However, the groups were produced sequentially from one common mortar batch rather than independently replicated batches, so the observed differences cannot be attributed solely to RTF configuration. The results do not establish statistical superiority, an optimized dosage, structural suitability, durability, environmental superiority, or a specific fiber–matrix mechanism.

6.7 Comparison with Previous Studies

Previous studies show that textile-fiber performance depends on feedstock, geometry, dosage, orientation, dispersion, matrix, and test method. Their commercial fibers, cut fabrics, carpets, and engineered textiles differ from the wastewater-recovered RTF investigated here (Rahman et al., 2022; Sasi et al., 2024; Tran et al., 2022).

The Mixed trend is compatible with reports that controlled fiber incorporation can preserve peak strength, while the Layered trend is compatible with the importance of reinforcement position and matrix penetration. Compatibility with a mechanism is not its demonstration.

The loose localized RTF region lacked the controlled continuity, thickness, orientation, and impregnation of engineered textiles or nonwovens (Koutas et al., 2019; Peled and Bentur, 2000; Sadrolodabaee et al., 2021a, 2021b).

Accordingly, published strength or durability benefits cannot be transferred directly to this feedstock and configuration.

6.8 Limitations

- Only three prism specimens were available per group, and all nine prisms originated from one common mortar batch; the groups were cast sequentially rather than as independently batched replicates. The paired compression halves were also not independent experimental units.
- Control supplied only two valid flexural results, and the Layered specimen with an improper failure mode was not identified.
- The unfiltered Control and Layered compression datasets did not pass the strict numerical ±10% individual-result evaluation criterion.
- The initial 28-day plan was not followed: flexure occurred at 56 days, microscopy at 95 days, and compression at 116 days. Storage after the documented 28-day water cure was not recorded.
- Handheld mixing, polystyrene molds, and manual compaction departed from standard preparation. Mixer speed, duration, energy, and compaction effort were not quantified.
- Only one RTF dosage was studied. Layer thickness, continuity, exact position, orientation relative to loading, and mass distribution among individual prisms were not documented sufficiently.
- The same material batch had prior micro-FTIR identification, but micro-FTIR was not repeated in this thesis. The 100 raw length values and a complete imaging protocol were unavailable for independent reanalysis.
- No standardized fresh-state, density, air-content, load–deflection, toughness, residual-strength, durability, or environmental assessment was performed.
- Selected two-dimensional microscope fields cannot quantify porosity, three-dimensional fiber distribution and orientation, bond strength, or interfacial chemistry.
- Flexural frame and load-cell details and the Zwick/Roell software environment were documented, but loading rates, calibration records, and the exact compression-frame model were unavailable.

7. Conclusions and Future Work

This thesis compared Mixed and Layered incorporation of wastewater-recovered RTF in mortar. Conclusions are restricted to the tested recovered-fiber batch, the nominal 1 wt% experimental designation, the single common mortar batch and sequential casting procedure, and the small specimen set.

7.1 Main Conclusions

1. The feedstock was physically heterogeneous in color, fluorescence, morphology, entanglement, and length. The visual 63% synthetic-like and 37% natural-like categories are not polymer fractions. The same batch had prior micro-FTIR identification, but micro-FTIR was not repeated as part of the present thesis.
2. Both RTF configurations could be prepared under the documented procedure. No standardized fresh-state result or three-dimensional distribution measurement established adequate workability or uniform dispersion.
3. Flexural differences were small and descriptive. Control had only two valid results, and the Layered mean is provisional because the improperly failed Layered specimen was not identified.
4. Compression results were also descriptive and paired within parent prisms. Mixed was 2.6% above the unfiltered Control mean, which does not establish strengthening; Layered was 16.1% below Control.
5. Selected microscope fields were consistent with different visible placement patterns, but did not establish chemical identity, porosity, bond strength, interfacial chemistry, three-dimensional distribution, or causal failure mechanisms.
6. Among the two RTF configurations, Mixed provided the more balanced descriptive specimen-level response. Because all groups were produced sequentially from one common mortar batch, the study does not provide independent batch replication and cannot isolate configuration from casting-order effects. No strengthening effect, optimized dosage, structural suitability, durability, or environmental superiority was established.

7.2 Practical Implications

The Mixed configuration is the more defensible starting point for further controlled laboratory research. The evidence does not support immediate product, non-structural, or structural-use recommendations.

Further Layered research should proceed only with defined position, thickness, continuity, orientation, and per-prism fiber mass, together with controlled matrix penetration and compaction.

RTF should be treated as a heterogeneous secondary feedstock, not a direct substitute for a standardized commercial fiber. Practical development requires reproducible recovery, conditioning, moisture control, batch characterization, mixing, and quality criteria.

7.3 Future Work

Future work should prioritize:

- prepare larger sets of independently mixed parent prisms and predefine validity, repeatability, and statistical-analysis rules;

- measure standardized flow, fresh density, air content, temperature, and relevant hardened transport properties;
- investigate several dosages and controlled length fractions at comparable, explicitly controlled effective w/c;
- characterize future batches directly by suitable spectroscopy and record moisture, diameter, surface condition, and residual contamination;
- record load–deflection response, toughness, fracture energy, residual strength, and crack development;
- quantify distribution and orientation and use SEM/EDS or another appropriate method where interface chemistry is relevant;
- for Layered specimens, control and report position, thickness, continuity, orientation, concentration, and number of layers;
- evaluate durability only after reproducible preparation and mechanical response are established;
- undertake application-specific testing only after repeatable laboratory performance is demonstrated; and
- perform life-cycle assessment only when reliable recovery, processing, transport, production, and end-of-life inventories are available.

References

Akyıldız, S.H., Bellopede, R., Sezgin, H., Yalcin-Enis, I., Yalcin, B. and Fiore, S. (2022) 'Detection and analysis of microfibers and microplastics in wastewater from a textile company', *Microplastics*, 1(4), pp. 572–586. https://doi.org/10.3390/microplastics1040040

Akyıldız, S.H., Sezgin, H., Yalcin, B. and Yalcin-Enis, I. (2023) 'Optimization of the textile wastewater pretreatment process in terms of organics removal and microplastic detection', Journal of Cleaner Production, 384, 135637. https://doi.org/10.1016/j.jclepro.2022.135637

Akyıldız, S.H., Yalcin Enis, İ., Sezgin, H., Bellopede, R., Fiore, S. and Yalcin, B. (2024) 'Separation and identification of microfibers in the wastewater of textile finishing process', *Politeknik Dergisi*, 27(6), pp. 2289–2295. https://doi.org/10.2339/politeknik.1310805

Akyıldız, S.H., Balestra, V., Drudi, L., Marini, P. and Bellopede, R. (2025a) 'Comparison of methodologies for microfiber analysis across different stages of wastewater from a textile dyeing company', *Journal of Hazardous Materials Advances*, 19, 100791. https://doi.org/10.1016/j.hazadv.2025.100791

Akyıldız, S.H., Sezgin, H., Özen, M.S. and Yalcin Enis, I. (2025b) 'Upcycling microfiber waste from wastewater into acoustic panels: A sustainable solution for sound absorption', *Environmental Research Letters*, 20(5), 054010. https://doi.org/10.1088/1748-9326/adc28b

Biyada, S., Merzouki, M. and Urbonavičius, J. (2023) 'New resources for sustainable thermal insulation using textile and agricultural waste in a new circular economy approach: An overview', *Processes*, 11(9), 2683. https://doi.org/10.3390/pr11092683

British Standards Institution (2016) *BS EN 196-1:2016: Methods of testing cement—Part 1: Determination of strength*. London: BSI.

Cai, Y., Mitrano, D.M., Heuberger, M., Hufenus, R. and Nowack, B. (2020) 'The origin of microplastic fiber in polyester textiles: The textile production process matters', *Journal of Cleaner Production*, 267, 121970. https://doi.org/10.1016/j.jclepro.2020.121970

Chan, C.K.M., Park, C., Chan, K.M., Mak, D.C.W., Fang, J.K.H. and Mitrano, D.M. (2021) 'Microplastic fiber releases from industrial wastewater effluent: A textile wet-processing mill in China', *Environmental Chemistry*, 18(3), pp. 93–100. https://doi.org/10.1071/EN20143

Chan, C.K.-M., Fang, J.K.-H., Fei, B. and Kan, C.-W. (2023) 'Microfibers release from textile industry wastewater effluents are underestimated: Mitigation actions that need to be prioritized', *Fibers*, 11(12), 105. https://doi.org/10.3390/fib11120105

Das, A.K., Hossain, M.F., Khan, B.U., Rahman, M.M., Asad, M.A.Z. and Akter, M. (2025) 'Circular economy: A sustainable model for waste reduction and wealth creation in the textile supply chain', *SPE Polymers*, 6(1), e10171. https://doi.org/10.1002/pls2.10171

Easton, T., Koutsos, V. and Chatzisymeon, E. (2023) 'Removal of polyester fiber microplastics from wastewater using a UV/H_2O_2 oxidation process', *Journal of Environmental Chemical Engineering*, 11(1), 109057. https://doi.org/10.1016/j.jece.2022.109057

European Environment Agency (2025) Circularity of the EU textiles value chain in numbers. EEA Briefing No. 03/2025. Copenhagen: European Environment Agency. https://doi.org/10.2800/5681501

European Parliament and Council of the European Union (2025) 'Directive (EU) 2025/1892 of the European Parliament and of the Council of 10 September 2025 amending Directive 2008/98/EC on waste', *Official Journal of the European Union*, L 2025/1892, 26 September. https://eur-lex.europa.eu/eli/dir/2025/1892/oj/eng

Fonseca, A., Ramalho, E., Gouveia, A., Henriques, R., Figueiredo, F. and Nunes, J. (2023) 'Systematic insights into a textile industry: Reviewing life cycle assessment and eco-design', *Sustainability*, 15(21), 15267. https://doi.org/10.3390/su152115267

Foti, D. (2013) 'Use of recycled waste PET bottles fibers for the reinforcement of concrete', *Composite Structures*, 96, pp. 396–404. https://doi.org/10.1016/j.compstruct.2012.09.019

Fraternali, F., Ciancia, V., Chechile, R., Rizzano, G., Feo, L. and Incarnato, L. (2011) 'Experimental study of the thermo-mechanical properties of recycled PET fiber-reinforced concrete', *Composite Structures*, 93(9), pp. 2368–2374. https://doi.org/10.1016/j.compstruct.2011.03.025

Haque, M.M., Kabir, A.T., Latifi, E.M., Mahmud, D.M.S., Hossain, M.R., Himu, H.A., Fatema, U.K. and Tareq, S.M. (2024) 'Microfiber prevalence and removal efficiency of textile effluent treatment plants in Bangladesh', *Journal of Hazardous Materials Advances*, 14, 100436. https://doi.org/10.1016/j.hazadv.2024.100436

Idrees, M., Saeed, F., Farooq, Z., Köksal, F. and Shi, J. (2023) 'Production of waste carpet fiber-reinforced concrete as sustainable material', *Journal of Building Engineering*, 77, 107499. https://doi.org/10.1016/j.jobe.2023.107499

Jayalath, A., Sofi, M., Ginigaddara, T., Gou, H., Mendis, P. and Aye, L. (2024) 'Mechanical properties and life cycle greenhouse gas analysis of textile waste fiber-based concrete', *Construction and Building Materials*, 428, 136267. https://doi.org/10.1016/j.conbuildmat.2024.136267

Juanga-Labayen, J.P., Labayen, I.V. and Yuan, Q. (2022) 'A review on textile recycling practices and challenges', *Textiles*, 2(1), pp. 174–188. https://doi.org/10.3390/textiles2010010

Koutas, L.N., Tetta, Z., Bournas, D.A. and Triantafillou, T.C. (2019) 'Strengthening of concrete structures with textile reinforced mortars: State-of-the-art review', *Journal of Composites for Construction*, 23(1), 03118001. https://doi.org/10.1061/(ASCE)CC.1943-5614.0000882

Lares, M., Ncibi, M.C., Sillanpää, M. and Sillanpää, M. (2018) 'Occurrence, identification and removal of microplastic particles and fibers in conventional activated sludge process and advanced MBR technology', *Water Research*, 133, pp. 236–246. https://doi.org/10.1016/j.watres.2018.01.049

Malchiodi, B., Cedillo-González, E.I., Siligardi, C. and Pozzi, P. (2022) 'A practical valorization approach in the production of cementitious composites containing textile finishing waste', Microplastics, 1(3), pp. 393–405. https://doi.org/10.3390/microplastics1030029

McCay, J. and Mehta, S. (2024) 'Microfiber fragment pollution: Sources, toxicity, strategies, and technologies for remediation', *Sustainability*, 16(7), 3077. https://doi.org/10.3390/su16073077

Mohtaram, F. and Fojan, P. (2025) 'From waste to value: Advances in recycling textile-based PET fabrics', *Textiles*, 5(3), 24. https://doi.org/10.3390/textiles5030024

Niinimäki, K., Peters, G., Dahlbo, H., Perry, P., Rissanen, T. and Gwilt, A. (2020) 'The environmental price of fast fashion', *Nature Reviews Earth & Environment*, 1(4), pp. 189–200. https://doi.org/10.1038/s43017-020-0039-9

Ochi, T., Okubo, S. and Fukui, K. (2007) 'Development of recycled PET fiber and its application as concrete-reinforcing fiber', *Cement and Concrete Composites*, 29(6), pp. 448–455. https://doi.org/10.1016/j.cemconcomp.2007.02.002

Peled, A. and Bentur, A. (2000) 'Geometrical characteristics and efficiency of textile fabrics for reinforcing cement composites', *Cement and Concrete Research*, 30(5), pp. 781–790. https://doi.org/10.1016/S0008-8846(00)00239-8

Rahman, S.S., Siddiqua, S. and Cherian, C. (2022) 'Sustainable applications of textile waste fiber in the construction and geotechnical industries: A retrospect', *Cleaner Engineering and Technology*, 6, 100420. https://doi.org/10.1016/j.clet.2022.100420

Ramasamy, R., Aragaw, T.A. and Balasaraswathi Subramanian, R. (2022) 'Wastewater treatment plant effluent and microfiber pollution: Focus on industry-specific wastewater', *Environmental Science and Pollution Research*, 29(34), pp. 51211–51233. https://doi.org/10.1007/s11356-022-20930-7

Sadrolodabaee, P., Claramunt, J., Ardanuy, M. and de la Fuente, A. (2021a) 'A textile waste fiber-reinforced cement composite: Comparison between short random fiber and textile reinforcement', *Materials*, 14(13), 3742. https://doi.org/10.3390/ma14133742

Sadrolodabaee, P., Claramunt, J., Ardanuy, M. and de la Fuente, A. (2021b) 'Characterization of a textile waste nonwoven fabric reinforced cement composite for non-structural building components', *Construction and Building Materials*, 276, 122179. https://doi.org/10.1016/j.conbuildmat.2020.122179

Sadrolodabaee, P., Claramunt, J., Ardanuy, M. and de la Fuente, A. (2021c) 'Mechanical and durability characterization of a new textile waste micro-fiber reinforced cement composite for building applications', *Case Studies in Construction Materials*, 14, e00492. https://doi.org/10.1016/j.cscm.2021.e00492

Sandin, G. and Peters, G.M. (2018) 'Environmental impact of textile reuse and recycling—A review', *Journal of Cleaner Production*, 184, pp. 353–365. https://doi.org/10.1016/j.jclepro.2018.02.266

Sasi, S., Joseph, P., Haigh, R., Sandanayake, M., Vrcelj, Z. and Yaghoubi, E. (2024) 'A review on the effects of waste textile polymer fiber on concrete strength: Exploring the key parameters', *Buildings*, 14(5), 1486. https://doi.org/10.3390/buildings14051486

Shirvanimoghaddam, K., Motamed, B., Ramakrishna, S. and Naebe, M. (2020) 'Death by waste: Fashion and textile circular economy case', *Science of the Total Environment*, 718, 137317. https://doi.org/10.1016/j.scitotenv.2020.137317

Talvitie, J., Mikola, A., Setälä, O., Heinonen, M. and Koistinen, A. (2017) 'How well is microlitter purified from wastewater? A detailed study on the stepwise removal of microlitter in a tertiary-

level wastewater treatment plant', *Water Research*, 109, pp. 164–172. https://doi.org/10.1016/j.watres.2016.11.046

Tang, K.H.D. (2023) 'State of the art in textile waste management: A review', *Textiles*, 3(4), pp. 454–467. https://doi.org/10.3390/textiles3040027

Tran, N.P., Gunasekara, C., Law, D.W., Houshyar, S., Setunge, S. and Cwirzen, A. (2022) 'Comprehensive review on sustainable fiber reinforced concrete incorporating recycled textile waste', *Journal of Sustainable Cement-Based Materials*, 11(1), pp. 28–42. https://doi.org/10.1080/21650373.2021.1875273

Tran, N.P., Gunasekara, C., Law, D.W., Houshyar, S. and Setunge, S. (2023) 'Utilization of recycled fabric-waste fibers in cementitious composite', *Journal of Materials in Civil Engineering*, 35(1), 04022372. https://doi.org/10.1061/(ASCE)MT.1943-5533.0004538

Wang, M., Yang, J., Zheng, S., Jia, L., Yong, Z.Y., Yong, E.L., See, H.H., Li, J., Lv, Y., Fei, X. and Fang, M. (2023) 'Unveiling the microfiber release footprint: Guiding control strategies in the textile production industry', *Environmental Science & Technology*, 57(50), pp. 21038–21049. https://doi.org/10.1021/acs.est.3c06210

Wang, S. and Salmon, S. (2022) 'Progress toward circularity of polyester and cotton textiles', *Sustainable Chemistry*, 3(3), pp. 376–403. https://doi.org/10.3390/suschem3030024

Wang, Y. (1999) 'Utilization of recycled carpet waste fibers for reinforcement of concrete and soil', *Polymer-Plastics Technology and Engineering*, 38(3), pp. 533–546. https://doi.org/10.1080/03602559909351598

Wojnowska-Baryła, I., Bernat, K., Zaborowska, M. and Kulikowska, D. (2024) 'The growing problem of textile waste generation—The current state of textile waste management', *Energies*, 17(7), 1528. https://doi.org/10.3390/en17071528

Xu, X., Hou, Q., Xue, Y., Jian, Y. and Wang, L. (2018) 'Pollution characteristics and fate of microfibers in the wastewater from textile dyeing wastewater treatment plant', *Water Science and Technology*, 78(10), pp. 2046–2054. https://doi.org/10.2166/wst.2018.476

Zhang, Y.-Q., Lykaki, M., Alrajoula, M.T., Markiewicz, M., Kraas

, C., Kolbe, S., Klinkhammer, K., Rabe, M., Klauer, R., Bendt, E. and Stolte, S. (2021) 'Microplastics from textile origin—Emission and reduction measures', *Green Chemistry*, 23(15), pp. 5247–5271. https://doi.org/10.1039/D1GC01589C

Zhou, H., Zhou, L. and Ma, K. (2020) 'Microfiber from textile dyeing and printing wastewater of a typical industrial park in China: Occurrence, removal and release', *Science of the Total Environment*, 739, 140329. https://doi.org/10.1016/j.scitotenv.2020.140329

Appendix

Appendix A — Supplementary RTF Characterization Images

Appendix A provides supplementary optical and ultraviolet-light images of recovered textile fibers. The images are qualitative documentation and do not establish polymer identity or composition.

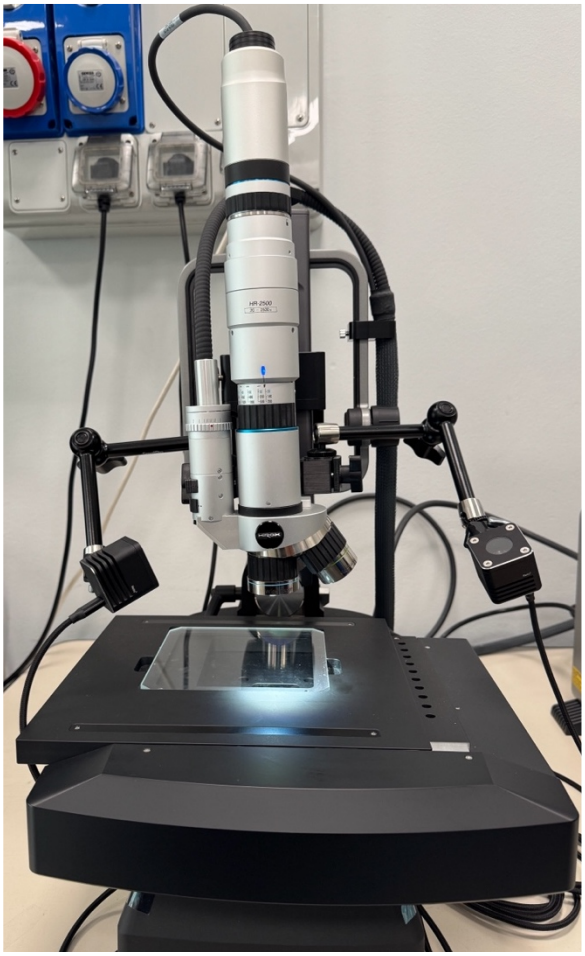
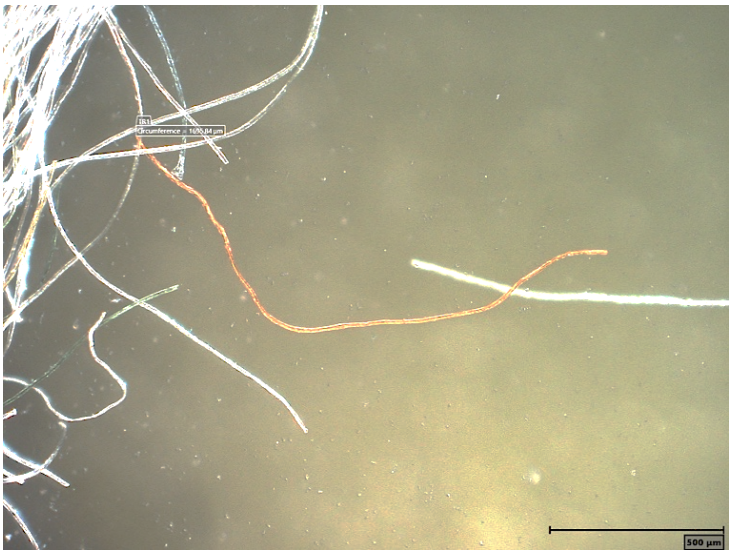
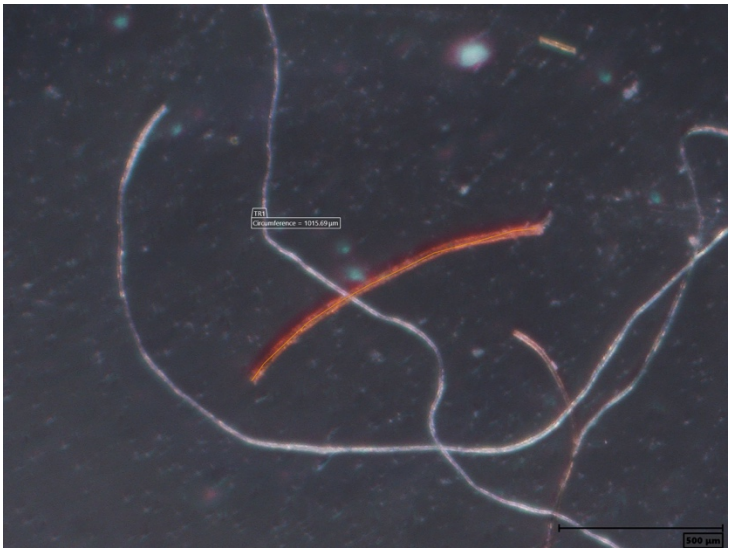
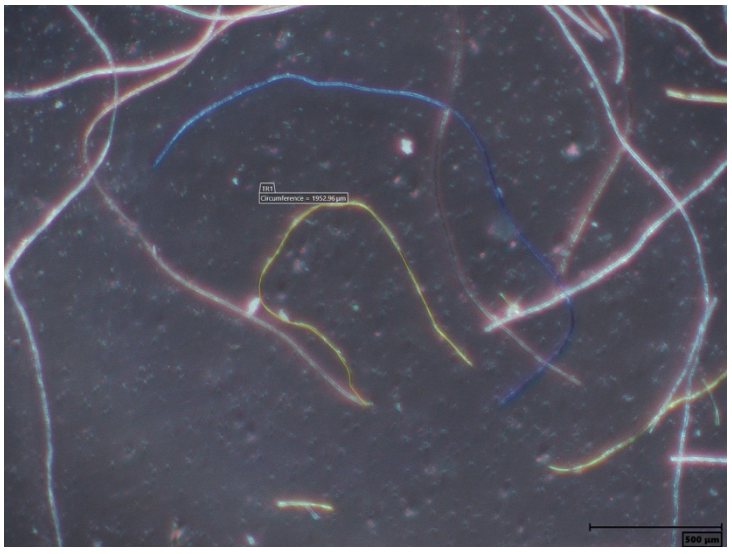


Figure A.1. HIROX digital microscope used for fiber and mortar-surface observations.


500 µm


Circumference = 1015.69 µm
500 µm


Circumference = 1952.96 µm
500 µm

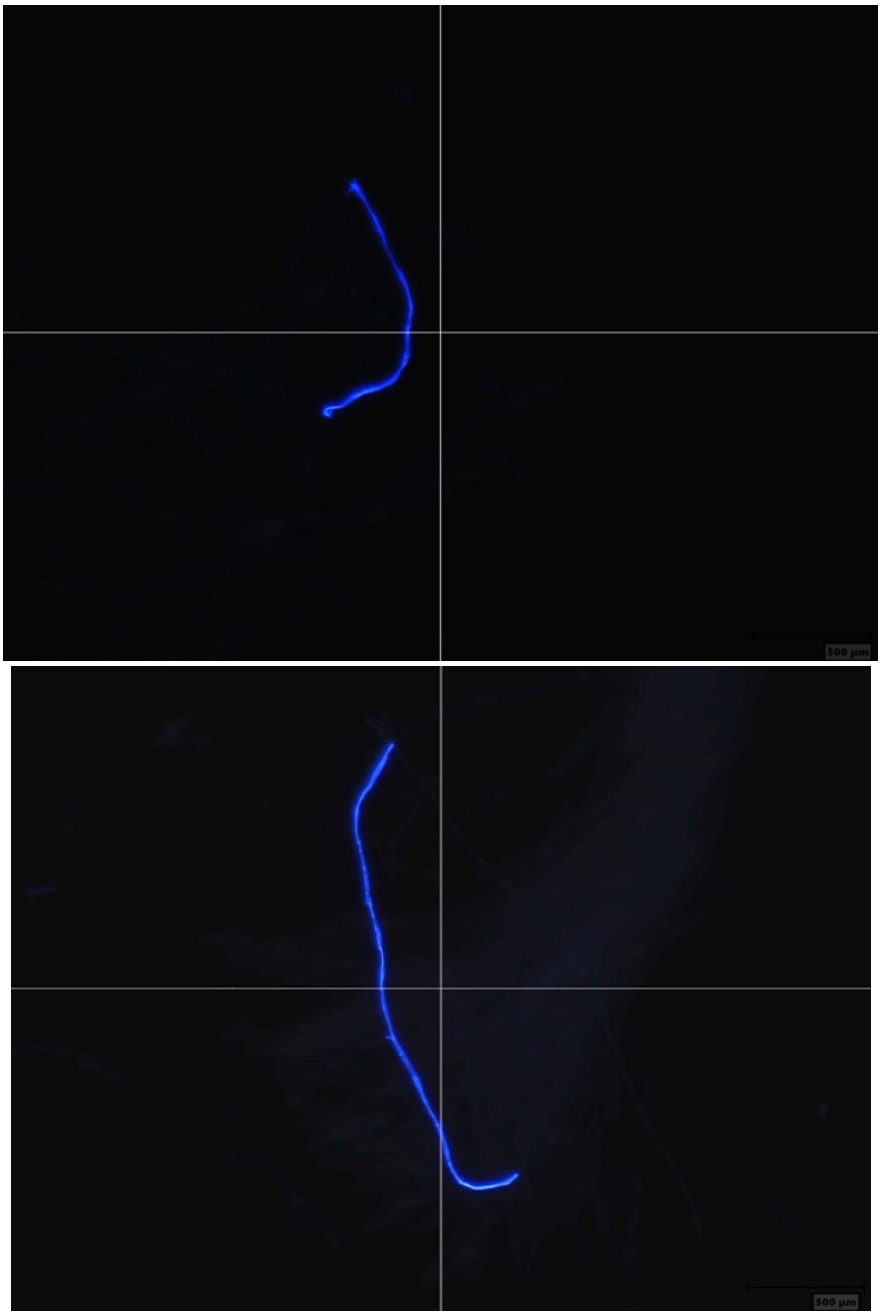


Figure A.2. Supplementary recovered-fiber fields; the original 500 µm scale bars and measurement overlays are retained where present.

Appendix B — Supplementary Specimen Preparation and Mechanical Testing Images

Appendix B provides qualitative photographic documentation of preparation, curing, flexural testing, compression testing, and post-test conditions. Screen images corroborate recorded loads and dates but are not substitute calibration records.



Figure B.1. Weighing of mortar constituents.



Figure B.2. Polystyrene prism molds.

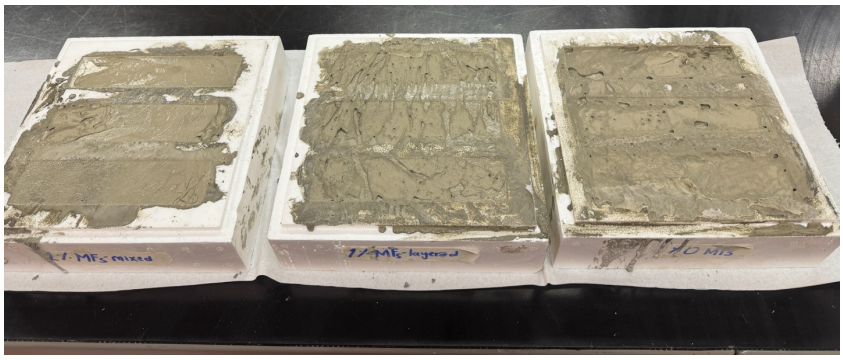


Figure B.3. Freshly cast Control, Mixed, and Layered prisms.

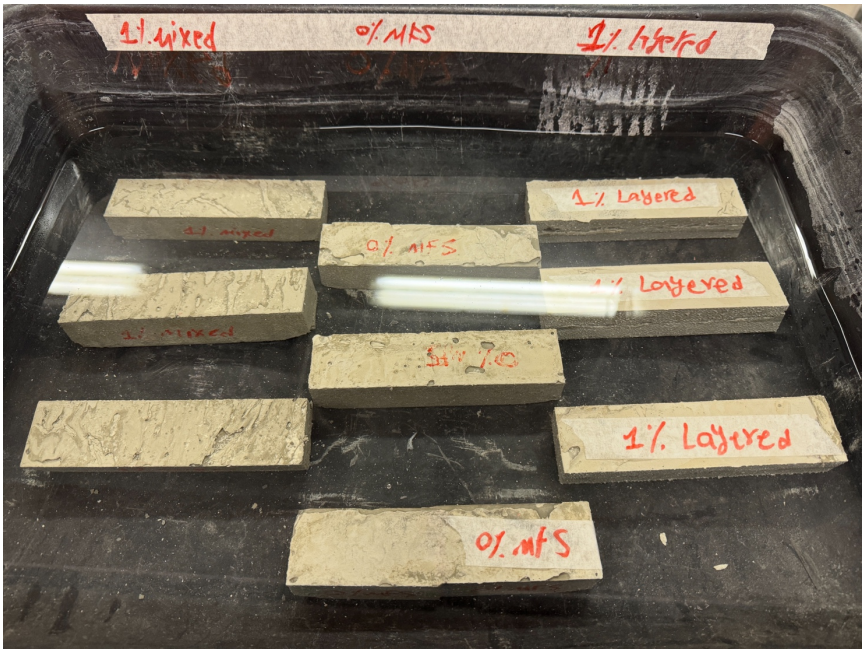


Figure B.4. Labeled prisms during water curing.



Figure B.5. Recorded flexural load–displacement display.

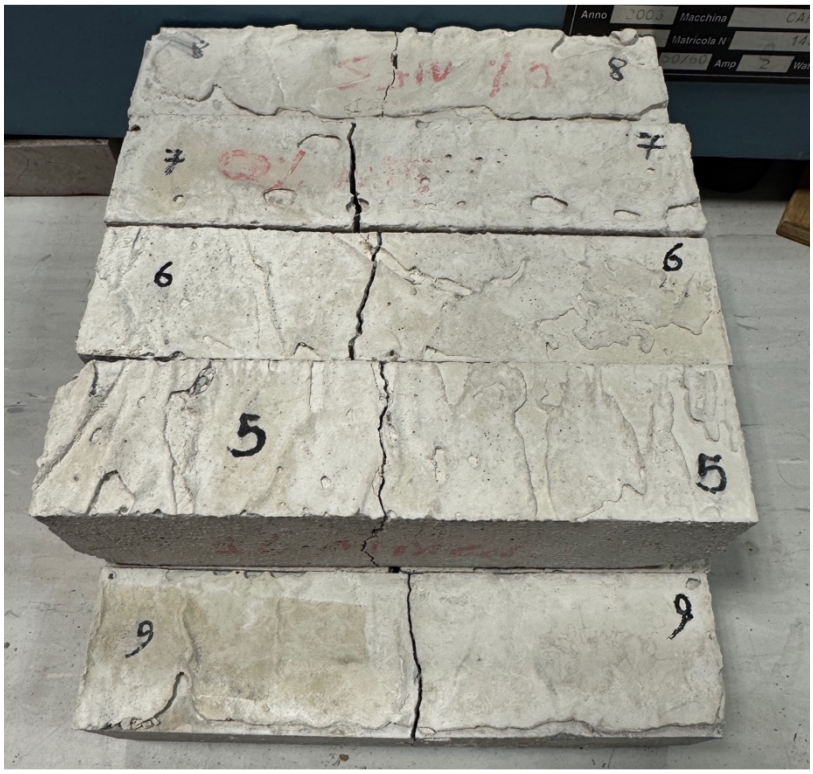


Figure B.6. Parent prisms after flexural testing.

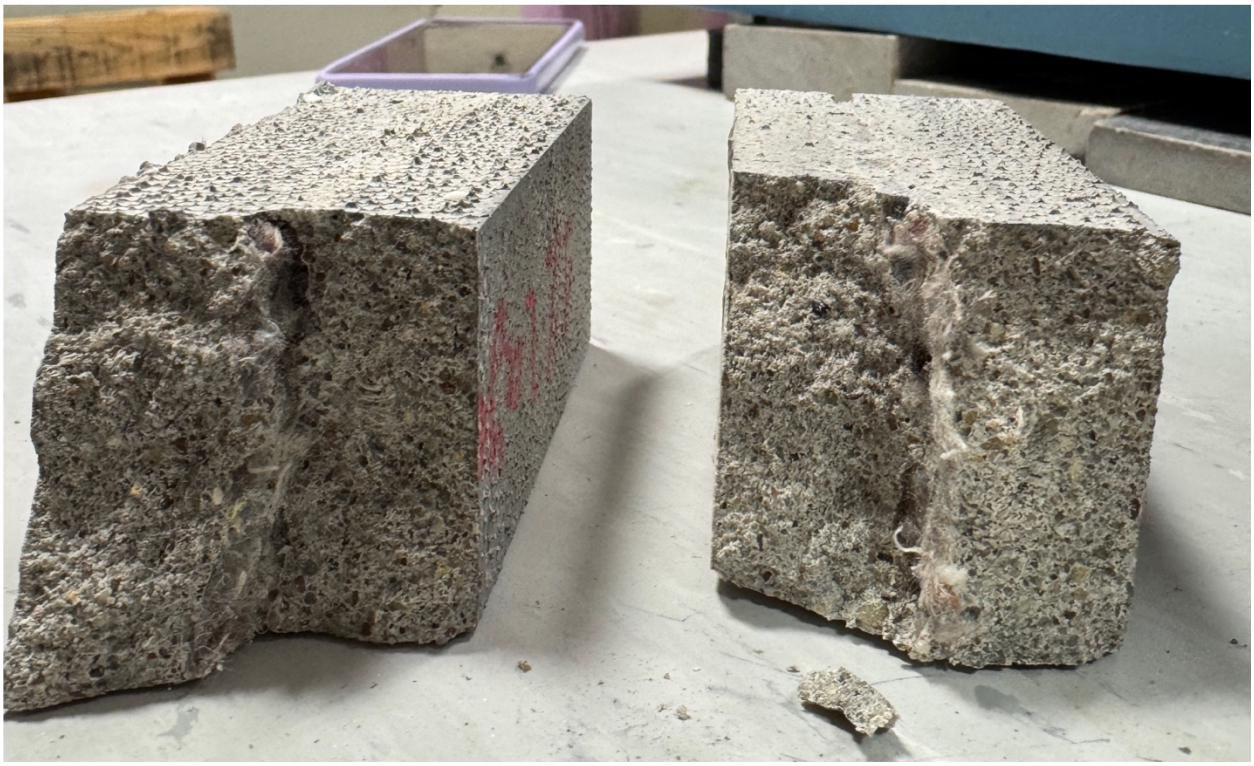


Figure B.7. Fractured surface with visible local fiber-rich material.



Figure B.8. Labeled half-prisms prepared for compression testing.



Figure B.9. Half-prism in the compression fixture.



Figure B.10. Zwick/Roell compression testing installation.

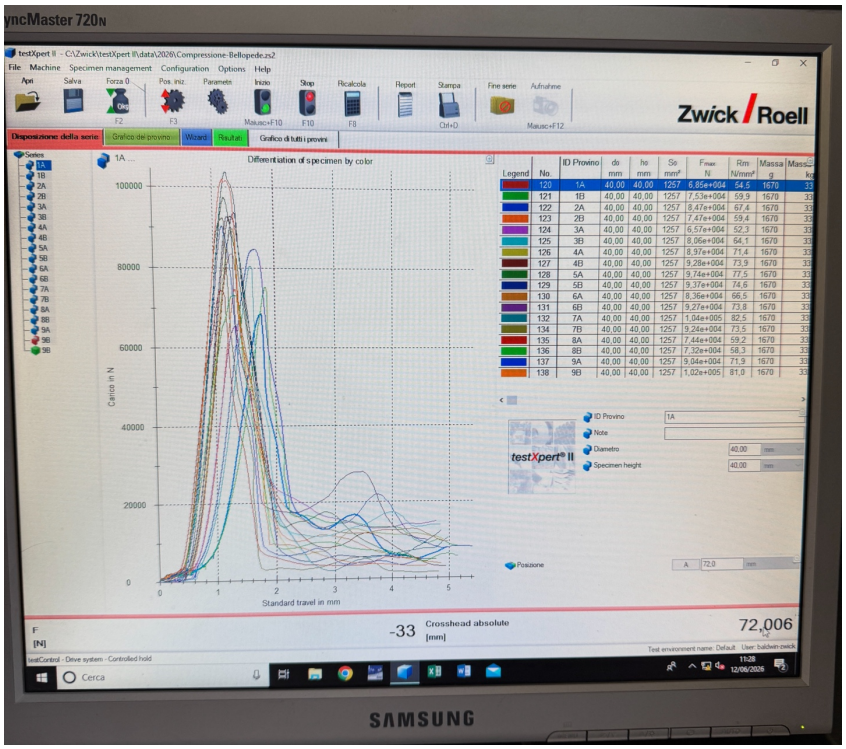


Figure B.11. testXpert II compression record showing the test date and peak-load results.

Appendix C — Supplementary Digital-Microscope Observations

Appendix C presents supplementary two-dimensional fields from Control, Layered, and Mixed specimens. They document visible surface features only and do not quantify porosity, three-dimensional fiber distribution, polymer identity, bond strength, or interfacial chemistry. Readable scale overlays were not present in these supplied source exports.

C.1 Control Specimens



Figure C.1. Supplementary Control fields showing matrix and aggregate features.

C.2 Layered 1% RTF Specimens



Figure C.2. Supplementary Layered fields showing localized loose-fiber regions.

C.3 Mixed 1% RTF Specimens

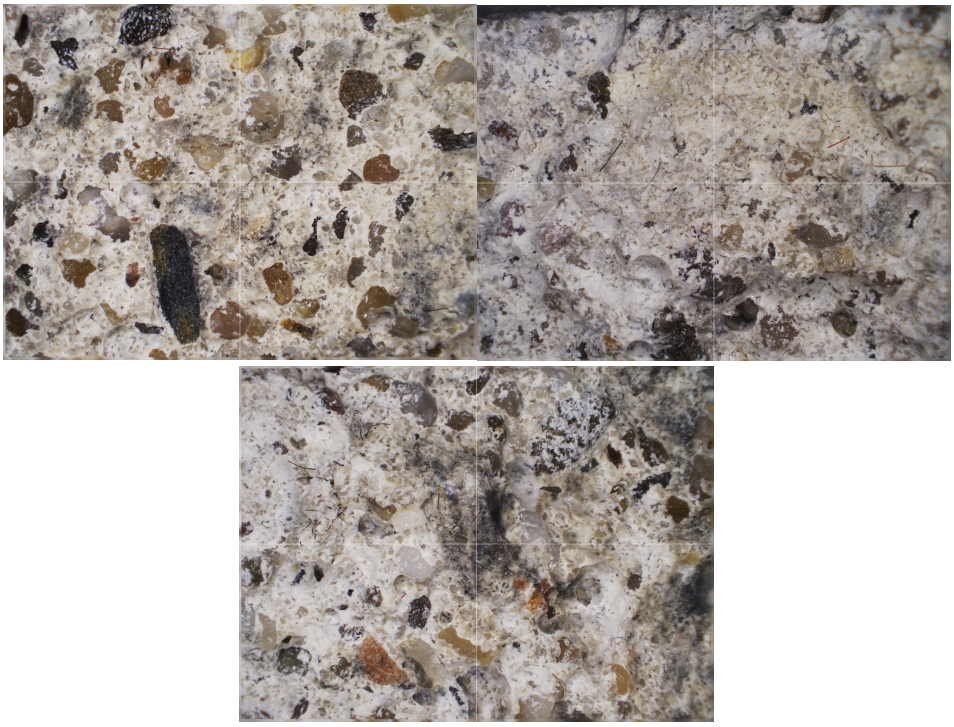


Figure C.3. Supplementary Mixed fields showing matrix-dominated regions and dispersed fiber-like elements.